

**Sensitivity Modeling sensitivities of BVOCs to different  
BVOC versions of MEGAN emission schemes in WRF-Chem (v3.6) to  
vegetation distributions and its impacts over East China**

<sup>1</sup>Mingshuai Zhang, <sup>1,2</sup>~~Chun~~<sup>2,3</sup>Chun Zhao\*, <sup>1</sup>Yuhan Yang, <sup>1</sup>Qiuyan Du,  
<sup>3</sup>~~Yonglin~~<sup>4</sup>Yonglin Shen, <sup>1</sup>Shengfu Lin, <sup>4</sup>~~Dasa~~<sup>5</sup>Dasa Gu, <sup>6</sup>Wenjing Su, <sup>7</sup>Cheng Liu

<sup>1</sup>School of Earth and Space Sciences, University of Science and Technology of China, Hefei, China

<sup>2</sup>CAS Center for Excellence in Comparative Planetology, University of Science and Technology of China, Hefei, China

<sup>3</sup>~~School~~<sup>3</sup>Frontiers Science Center for Planetary Exploration and Emerging Technologies, University of Science and Technology of China, Hefei, China

<sup>4</sup>~~School~~ of Geography and Information Engineering, China University of Geosciences, Wuhan 430074, China

<sup>4</sup>~~Division~~<sup>5</sup>Division of Environment and Sustainability, Hong Kong University of Science and Technology, Clear Water Bay, Hong Kong SAR, China

<sup>6</sup>Department of Environmental Science and Engineering, University of Science and Technology of China, Hefei, China

<sup>7</sup>Department of Precision Machinery and Precision Instrument, University of Science and Technology of China, Hefei, China

Manuscript for submission to *Geoscientific Model Development*

\*Corresponding author: Chun Zhao (chunzhao@ustc.edu.cn)

**Key points:**

1. Modeling performance of BVOC and its impact over East China using different versions (v1.0, v2.0, v3.0) of Model of Emissions of Gases and Aerosols from Nature (MEGAN) in WRF-Chem(v3.6) are examined and documented.
2. Three versions of MEGAN show different sensitivity to vegetation distributions and simulate different seasonal variations of BVOC emissions over East China.
3. Temperature-dependent factor dominates the seasonal change of activity factor in all three versions of MEGAN, while the different response to the change of leaf area index

带格式的: 居中

带格式的: 行距: 单倍行距

带格式的: 行距: 单倍行距

带格式的: 字体: 倾斜

37 determines the difference among the three versions in seasonal variation of BVOC  
38 emissions.  
39 4. The surface ozone concentration can be significantly affected by BVOC emissions  
40 over East China, but the impact is sensitive [to](#) the MEGAN versions.

## Abstract

Biogenic volatile organic compounds (BVOCs) simulated by current air quality and climate models still have large uncertainties, which can influence atmosphere chemistry and secondary pollutant formation ~~over East China.~~ These ~~uncertainties~~ modeling sensitivities are ~~generally resulted from~~ primarily due to two sources. One ~~is~~ originates from different ~~biogenic emission schemes coupled in model, representing for different~~ treatments ~~of in the~~ physical and ~~chemistry progresses during the emissions~~ chemical processes associated with the emission rates of BVOCs. The other is ~~from errors in the~~ biased distributions specification of vegetation types and their distribution over a specific region. In this study, the version of Weather Research and Forecasting model coupled with Chemistry (WRF-Chem) updated by the University of Science and Technology of China (USTC version of WRF-Chem) from the public WRF-Chem(v3.6) is used. The modeling results over East China with different versions (v1.0, v2.0, v3.0) of Model of Emissions of Gases and Aerosols from Nature (MEGAN) in WRF-Chem are examined and documented. Sensitivity experiments with these three versions of MEGAN and two vegetation datasets are conducted to investigate the difference of three MEGAN versions in modeling ~~biogenic VOCs~~ BVOCs and its dependence on the vegetation distributions. The experiments are also conducted for spring (April) and summer (July) to examine the seasonality of the modeling results. The results indicate that MEGANv3.0 simulates the largest amount of biogenic isoprene emissions over East China. The different performance among MEGAN versions is primarily due to their different treatments of applying emission factors and vegetation types. In particular, the results highlight the importance of considering sub-grid vegetation fraction in estimating BVOCs emissions ~~over East China with large area of urbanization.~~ Among all activity factors, temperature-dependent factor dominates the seasonal change of activity factor in all three versions of MEGAN, while the different response to the leaf area index (LAI) change determines the difference among the three versions in seasonal variation of BVOC emissions. The simulated surface ozone concentration due to BVOCs can be significantly different (ranging from 1 ppbv to more than 10 ppbv in some regions) among the experiments with three versions of MEGAN, which is mainly due to their impacts on surface VOCs and NO<sub>x</sub> concentrations. This study suggests that there is still large uncertain range in modeling BVOCs Theoretically MEGANv3.0 that is coupled with the land surface scheme and considers the sub-grid vegetation effect should overcome previous versions of MEGAN in WRF-Chem. However, considering uncertainties of retrievals and anthropogenic emissions over East China, it is still difficult to apply satellite retrievals of formaldehyde and/or limited sparse in-situ observations to constrain the uncertain parameters or functions in BVOCs emission schemes and their impacts on photochemistry and ozone production. More accurate vegetation distribution and measurements of biogenic emission ~~fluxes~~ fluxes and species ~~concentrations~~ concentrations are still needed to better evaluate ~~the model performance~~ and ~~reduce the uncertainties~~ optimize models.

带格式的: 字体: + 西文正文 (等线), 五号

84

85

## 1. Introduction

Volatile organic compounds (VOCs) in the atmosphere are from biogenic and anthropogenic sources. Previous studies have indicated that biogenic emission is the dominant source of VOCs, accounting for about 90% of total emissions at global scale (Guenther et al., 1995). Biogenic VOCs (BVOCs) ~~plays~~ a critical role in atmosphere chemistry because some species such as isoprene and monoterpenes are reactive, and can participate in atmospheric photochemical reactions. Therefore, BVOCs could have significant impact on the formation of ozone and secondary organic aerosol (SOA) and ultimately air quality and climate change (Pierce et al., 1998; Carslaw et al., 2000; Poisson et al., 2000; Zhang et al., 2000; Carlton et al., 2009; Brown et al., 2013; Hantson et al., 2017). Among the BVOCs species, isoprene is one of the key identified species that dominates the BVOCs emissions. Global estimation also shows that biogenic isoprene emission is approximately half of total BVOCs emissions (Guenther et al., 2012).

Due to the importance of BVOCs for atmospheric environment, progress has been made extensively in modeling BVOCs emission and its impacts regionally and globally over the past several decades (Geron et al., 1994; Guenther et al., 1995; Niinemets et al., 1999; Arneth et al., 2007). BVOCs emissions are normally estimated with numerical schemes, such as the Seasonal Isoprene synthase Model-Biochemical Isoprenoid biosynthesis Model (SIM-BIM) (Lehning et al., 2001; Zimmer et al., 2003), the Biogenic Emission Inventory System (BEIS)(Pierce et al., 1998), the Global Biosphere Emissions and Interactions System (GloBEIS3) (Yarwood et al., 2002), the semi-empirical BVOC emission model (seBVOC) (Stewart et al., 2003), and the Model of Emissions of Gases and Aerosols from Nature (MEGAN) (Guenther, 2006; Guenther et al., 2012; Zhao et al., 2016; Jiang et al., 2018). MEGAN is one of the widely used emission schemes for estimating BVOCs emissions under different environmental conditions, and has been coupled with multiple chemical transport models to include the ~~contributions~~ ~~impact~~ of BVOCs ~~to the variations of~~ air pollutants (Levis et al., 2003; Yang et al., 2011; Ghude et al., 2013; Situ et al., 2013; Tie et al., 2013; Li and

Xie, 2014; Forkel et al., 2015; Kota et al., 2015; Liu et al., 2018; Wu et al., 2020).

However, there still remain larger [uncertaintiesmodeling sensitivities](#) in the estimation of BVOCs emission with MEGAN, due to the uncertain emission rates of some compounds, the limited knowledge of environmental activity factors controlling the BVOCs emissions, the accuracy of vegetation distributions, and etc. (Guenther, 2013).

WRF-Chem (Weather Research and Forecasting model coupled with Chemistry) is an online coupled meteorology and chemistry model that can simulate meteorology fields and chemical species simultaneously (Grell et al., 2005; Fast et al., 2006). The MEGAN scheme is widely used for estimating biogenic emissions online with WRF-Chem (Jiang et al., 2012a; Wang et al., 2015; Abdi-Oskouei et al., 2018; Wei et al., 2018; Arghavani et al., 2019; Safronov et al., 2019; Visser et al., 2019; Li et al., 2020; Yin et al., 2020). The public versions (v4.2 and older) of WRF-Chem include the first MEGAN version (referred to as MEGANv1.0 hereafter) (Guenther et al., 1995) and the second version (referred to as MEGANv2.0 hereafter) (Guenther, 2006). The first version is an earlier scheme with simple canopy treatment and chemical mechanism, considering only the environmental effects from light and temperature on emission flux, and therefore is mainly used in previous studies (e.g., (Guenther et al., 1996; Derognat et al., 2003) but not often in recent studies. Comparatively, MEGANv2.0 is more commonly used for calculating the BVOC emissions with WRF-Chem recently (Geng et al., 2011; Jiang et al., 2012b; Zhang et al., 2015; Zhou et al., 2017) due to its treatment of additional chemical compounds and plant types for emissions. It also considers more complex environmental controlling processes. MEGANv2.1 (Guenther et al., 2012) was recently coupled with WRF-Chem embedded in the CLM4 land surface scheme (Zhao et al., 2016), so that MEGAN obtains the meteorological fields that are calculated online and the consistent vegetation types from the land surface scheme. Although all these three MEGAN versions were coupled in WRF-Chem and used for estimating BVOCs emissions, so far the difference among these MEGAN versions in terms of modeling BVOCs emission and its impacts in WRF-Chem is not examined and documented.

With the rapid increase in economic development during the past several decades,

East China has become the most prosperous and developed region of China's economy. More and more air pollutants and precursors are emitted into the atmosphere over the region. Previous studies have found that BVOCs play important roles on air pollutant production over East China (e.g., (Han et al., 2005; Wei et al., 2007; Wang et al., 2008; Fu et al., 2010; Zheng et al., 2010; Li et al., 2015a; Li et al., 2015b). Tie et al. (2013) found that the ozone formation was strongly VOC-limited in Shanghai of East China and its production could partly attributed to the biogenic emission of isoprene. Jiang et al. (2012b) investigated the impacts of local biogenic and anthropogenic emissions to the daytime mean ozone mixing ratios over East China using WRF-Chem with MEGANv2.0. Geng et al. (2011) applied WRF-Chem with MEGANv2.0 for studying the effect of isoprene on ozone formation in Shanghai, and they found that the BVOCs from the major forest surrounded have significant impact on ozone production through two different mechanisms. Li et al. (2017a) employed WRF-Chem with MEGANv2.0 to estimate the relative contribution of biogenic and anthropogenic sources to ozone concentration over East China, and concluded that the BVOCs contributed significantly to the background ozone concentration. Wang et al. (2019) founded that the ozone concentration in south of Shanghai can be enhanced significantly due to the mixing of the emissions of BVOCs from the forest and precursors from the ships.

Since the WRF-Chem model with different MEGAN versions has been widely used for studying the impacts of BVOCs on air quality over East China while the performance of different MEGAN versions in WRF-Chem has not been examined, this study aims to ~~investigated~~[investigate](#) the difference of MEGAN versions in terms of modeling BVOCs, focusing on biogenic isoprene, and its impact on ozone concentration over East China. This study updates the MEGANv2.1 coupled by Zhao et al. (2016) to the latest version MEGANv3.0 ([Jiang et al., 2018](#)) (see details in Section 2.2), and analyzes the difference of WRF-Chem modeling results with MEGANv1.0, MEGANv2.0, and MEGANv3.0. Numerical experiments are conducted for April and July of 2015 to reflect the seasonal variation of biogenic isoprene emissions and its potential impacts. In order to examine the different sensitivities of MEGAN versions in WRF-Chem to vegetation distributions, two land-use datasets are adopted in this study,

which are USGS24 (United States Geological Survey 24 categories classification) and MODIS2015 (a new dataset derived from the satellite retrievals in this study representing the land-use condition of 2015). [In summary, this study documents the different performance among different versions of MEGAN and its impacts on ozone and other chemical compounds, which can provide the WRF-Chem community more comprehensive analysis to understand the mechanisms of modeling sensitivities in BVOCs among different versions of MEGAN in WRF-Chem and vegetation distributions. The different response to seasonal change and vegetation distributions are also quantified. On the other hand, modeling sensitivity analysis also provides more information about what and where to measure for better constraining the modeling of BVOCs over East China.](#) The paper is organized as following. Section 2 describes the numerical experiments and methods. The results and discussions are presented in Section 3. A summary is provided in Section 4.

## **2. Methodology**

### **2.1. WRF-Chem**

The version of WRF-Chem updated by University of Science and Technology of China (USTC version of WRF-Chem) is used in this study. Compared with the publicly released version, this USTC version of WRF-Chem includes some additional functions such as the MEGAN scheme implemented in the land surface model (Zhao et al., 2013a; Zhao et al., 2013b; Zhao et al., 2014; Zhao et al., 2016). The configuration of WRF-Chem in this study is similar to that used by (Zhao et al., 2016). In brief, the CBM-Z photochemical mechanism (Zaveri and Peters, 1999) is selected to simulate the gas-phase chemistry that contains 55 prognostic species and 134 reactions. The photolysis rates is computed by the Fast-J radiation parameterization (Wild et al., 2000), and the Yonsei University (YSU) scheme (Hong et al., 2006) is for planetary boundary layer (PBL) parameterization. All of the WRF-Chem simulations use the Morrison two-moment scheme (Morrison et al., 2009) for cloud physics, the Monin–Obukhov similarity theory (Paulson, 1970) for surface layer, the Kain–Fritsch scheme (Kain, 2004) to simulate sub-grid scale clouds and precipitation and the rapid radiative transfer



parameterization (RRTMG) for both longwave and shortwave radiation (Iacono et al., 2008). In order to show the design of experiment clearly, all configurations are listed in Table 1.

## 2.2 MEGAN implemented in WRF-Chem

MEGAN is a widely used scheme for calculating biogenic emissions from terrestrial system to atmosphere with the impact from different environmental conditions, such as radiation, temperature, soil moisture, and leaf area. Three versions of MEGAN online coupled with WRF-Chem are used in this study, MEGANv1.0, MEGANv2.0, and MEGANv3.0 that is updated from MEGANv2.1 as implemented by (Zhao et al., 2016) according to the changes made by Jiang et al. (2018)

## 2.2 MEGAN implemented in WRF-Chem

MEGAN is a widely used scheme for calculating biogenic emissions from terrestrial system to atmosphere with the impact from different environmental conditions, such as radiation, temperature, soil moisture, and leaf area. However, different versions of MEGAN implement different treatments for calculating emission rates and environmental forcing, and therefore, the detailed difference of these versions of MEGAN in WRF-Chem and their impacts on modeling results needs to be quantified. Three versions of MEGAN (MEGANv1.0, MEGANv2.0, and MEGANv3.0) online coupled with WRF-Chem are investigated in this study. The details about these three different versions are described below.

~~and the technical description of CLM4.0 (Oleson et al., 2010).~~

MEGAN in WRF-Chem estimates biogenic emission ( $F_i$ ) of different chemical compounds ( $i$ ) based on emission factors ( $\varepsilon_i$ ) ( $\mu\text{g m}^{-2}\text{h}^{-1}$ ), activity factors ( $\gamma_i$ ) that is controlled by environmental conditions, and the ~~loss~~ and production rate within the plant canopy ( $\rho$ ).

$$F_i = \varepsilon_i \times \gamma_i \times \rho \quad (1)$$

Where  $\varepsilon_i$  is a plant function type (PFT) weighted value that is calculated by PFT specific emission factor  $\varepsilon_{i,j}$  and grid box area coverage fraction  $f_{PFT(j)}$  of PFT( $j$ ),

i.e.,  $\varepsilon_i = \sum \varepsilon_{i,j} f_{PFT(j)}$  and  $\gamma_i$  is the product of each activity factor such as leaf-level photosynthetic photon flux density (PPFD)( $\gamma_p$ ), temperature( $\gamma_t$ ), leaf area index (LAI) ( $\gamma_{LAI}$ ) and leaf age( $\gamma_a$ ), i.e.,  $\gamma_i = \gamma_{LAI} \gamma_p \gamma_t \gamma_a$

MEGANv1.0 is the first model version coupled in WRF-Chem. It considers only the response of emission to radiation and temperature. The mechanism of environmental impact is very simple compared with the later versions. For emission factors, MEGANv1.0 follows the land surface scheme with 24 land use types and prescribes emission factor for each land-use type (Fig. 2). It groups the 24 land-use types into the 6 plant categories (urban or bare soil, agriculture, grassland, deciduous forest, mixed forest, and other natural land) for calculating biogenic emission activity factor.

Guenther [et al.](#) (2006) introduced MEGANv2.0 that is a major update from the previous version. ~~In the version of WRF-Chem used in this study, it is separated to estimate~~The emission factor ~~at of BVOCs for~~ each grid cell ~~for isoprene and other BVOCs, respectively, although the public offline MEGANv2.0 has the option to calculate isoprene emission factor based on PFT. In WRF-Chem, the emission factor is can be prescribed for isoprene emission at each grid cell, and/or calculated for other BVOCs using PFT-specified emission factors and PFT cover database. Thewith prescribed vegetation distributions can also be customized.~~distribution and emission factor for each PFT. For activity factor, the impacts of PPFD, temperature, monthly LAI, leaf age, soil moisture, and solar radiation on biogenic emissions are taken into account (Guenther, [et al.](#), 2006). ~~However, there are some shortcomings in~~ Different from the released offline MEGANv2.0 ~~implemented in public version, after coupled with WRF-Chem, MEGANv2.0 reads emission factor at each grid cell for isoprene and calculate emission factors for other BVOCs based on PFT's and PFT-specified emission factor at each grid cell. The vegetation distribution at each grid cell used in MEGANv2.0 in WRF-Chem includes only 4 dominant PFT at each grid cell and is prescribed differently from the one used in the land surface scheme (e.g., 24 land-use types). In addition, the MEGANv2.0 coupled with the publicly released versions of~~

WRF-Chem. ~~MEGANv2.0~~ uses the monthly mean surface air temperature, LAI and solar radiation from the climatological database that may not be consistent with the meteorological fields during ~~the simulation. In addition, the vegetation distribution at each grid cell used in MEGANv2.0 (only 4 dominant PFT) is prescribed as different from the one used in the land surface scheme (e.g., 24 land use types). Zhao et al. (2016) implemented MEGANv2.1 into CLM4.0 in WRF-Chem so that the biogenic emission scheme and the land surface scheme can use the consistent distributions of vegetation type, surface air temperature, LAI and solar radiation. For emission factors, MEGANv2.1 defines as the net primary emission that escaped into the atmosphere and it does not contain the downward flux of chemicals from above canopy, while MEGAN 2.0 defines as the total flux of chemical compounds, detailed in simulation.~~

The MEGANv3.0 employed in this study is updated from MEGANv2.1 as implemented by Zhao et al. (2016). Zhao et al. (2016) implemented MEGANv2.1 into CLM4.0 in WRF-Chem so that biogenic emission and land surface processes can use consistent distributions of meteorological fields such as land-use type, surface air temperature, LAI, and solar radiation, which is significantly different from previous versions (v1.0 and v2.0) in terms of scheme structure because the coupling of previous versions of MEGAN is independent of land surface scheme. Compared to the widely used MEGANv2.0 in WRF-Chem that defines emission factor as the total flux of chemical compounds, MEGANv2.1 defines emission factor as the net primary emission that escaped into the atmosphere and it does not contain the downward flux of chemicals from above canopy, as detailed in Zhao et al. (2016). In addition, MEGANv2.1 can also consider sub-grid vegetation distributions, which is different from previous versions that generally apply dominant vegetation type in each grid for BVOC emission calculation. The primary update in MEGANv3.0 from MEGANv2.1 is to consider drought activity factor as one of environmental forcing. It is implemented in this study to include the effect of drought on biogenic emissions following the drought feedback mechanism introduced by Jiang et al. (2018) and the technical description of CLM4.0 (Oleson et al., 2010).-

Recently, Jiang et al. (2018) established the relationship between photosynthesis

and water stress and the BVOCs emissions that is not included in MEGANv2.1 in WRF-Chem. They presented a more sophisticated mechanistic representation of BVOCs emission in MEGAN (referred to as MEGANv3.0 hereafter) to simulate the impact of drought on biogenic isoprene emissions. Following Jiang et al. (2018), the MEGANv2.1 in WRF-Chem is updated to MEGANv3.0 in this study to include the effect of drought on biogenic emissions, in which the new drought activity factor  $\gamma_{d,isoprene}$  is calculated as the following formula:

$\gamma_{d,isoprene} = 1 - \frac{(\beta_t - 0.6)}{\alpha}$  They presented a more sophisticated mechanistic representation of BVOCs emission in MEGAN to simulate the impact of drought on biogenic isoprene emissions. The new drought activity factor  $\gamma_{d,isoprene}$  is calculated as the following formula:

$$\gamma_{d,isoprene} = 1 \quad (\beta_t > 0.6)$$

$$\gamma_{d,isoprene} = V_{cmax}/\alpha \quad (\beta_t < 0.6, \alpha = 37) \quad (2)$$

where  $\alpha$  is an empirical and regionally applicable value derived from field measurements at observation site in Missouri Ozarks AmeriFlux site (MOFLUX) to limit and modify the isoprene emission due to the drought force. Therefore, the value of  $\alpha$  may not be suitable for China. However, due to the lack of observations in China, the default  $\alpha$  value is used in this study.  $V_{cmax}$  is the photosynthetic enzyme activity, and  $\beta_t$  is the soil water stress function calculated as following:

$$\beta_t = \sum w_i r_i \quad (3)$$

where  $w_i$  is the wilting factor based on soil water potential at each soil layer, and  $r_i$  is the fraction of roots in soil layer. More details can be found in the CLM4.0 technical notes (Oleson et al., 2010). It is noteworthy that the major difference between MEGANv3.0 and previous versions is primarily caused by the difference between MEGANv2.1 and previous versions as discussed above instead of drought effect.

### 2.3 Vegetation distribution

Zhao et al. (2016) suggested that the distributions of vegetation types play an important role in determining regional emissions of BVOCs with MEGAN. Two

vegetation datasets are used to examine the sensitivities of BVOCs emissions with different MEGAN versions to vegetation distributions. One is the default land cover dataset (USGS24) used in WRF-Chem (referred to as VEG-USGS hereafter), which generally represents the land cover information for 1990s over East China (Loveland et al., 2000). It is converted to 16-PFT data set in CLM4.0 (~~referred to as VEG-USGS hereafter~~) following the table derived by Bonan (1996) as Zhao et al. (2016). Specific descriptions of legend and class of the land cover data are listed in the Table 42. Another land cover dataset is derived from the [Moderate Resolution Imaging Spectroradiometer \(MODIS\)](#) retrievals in 2015 (referred to as VEG-2015 hereafter~~;~~) [and converted to 16-PFT data using the same method as VEG-USGS](#), which has the horizontal resolution of 1 km over ~~entire~~[all of](#) China. VEG-2015 were reclassified on the existing products of 2015, including GFSAD1000 (Cropland Extent 1km Crop Dominance, Global Food-Support Analysis Data) (Thenkabail et al., 2012), and MODIS MCD12Q1 (MODIS Land Cover Type Yearly Global 500m) product (Friedl et al., 2002). For MCD12Q1 product, there are six different classification schemes (Gregorio, 2005), in which the two schemes of FAO (Food and Agriculture Organization) LCCS (Land Cover Classification System) land cover and FAO LCCS surface hydrology were used. [Theoretically, VEG-2015 should be more representative for the reality in 2015, particularly for East China with intensive urban expansion since 2000s.](#)

Figure 1 shows the spatial distributions of the dominant PFT within each model grid cell (see details in Section 2.4) over East China from these two vegetation datasets. It is apparent that VEG-2015 is much different from VEG-USGS. The Z-shaped urban belt of Yangtze River Delta region is evident in VEG-2015 but not in VEG-USGS. Not only the dominant PFT but also the sub-grid distributions of PFTs are different between the two datasets (not shown). [Table 4\), all these can show that VEG-2015 is more conform with the land cover in recent China than VEG-USGS.](#) Table 2 illustrates the percentage of each PFT averaged over the simulated domain from the two vegetation data sets. For example, the fraction of needleleaf evergreen tree that is a major species of biogenic emission range from 7.9% in VEG-USGS to 1.7% in VEG-2015, and the fraction of bare soil is nearly twice that of VEG-USGS. The emissions of BVOCs from

MEGAN could be significantly different due to this difference. The sensitivity of MEGAN-estimated BVOCs ~~emission~~emissions to ~~different~~these two vegetation distributions may also be different ~~for~~due to the different treatment of vegetation type in three versions of MEGAN used in this study.

## 2.4 Numerical experiments

In this study, the simulations are conducted with a horizontal resolution of 12km and 120×100 grid cells (109.3°E~125.6°E, 25.4°N~36.4°N; Fig. S1 in the supporting material) over East China. The simulation periods are April and July of 2015 representing one month of spring and summer, respectively, to reflect the seasonal variation of biogenic emission. The quasi-global WRF-Chem simulation with 360×145 grid cells (180°W~180°E, 67.5°S~77.5°N) at the 1°×1° horizontal resolution is used to provide the chemical boundary condition. The meteorological initial and lateral boundary conditions are obtained from the NCEP Final reanalysis (FNL) data with 1°×1° resolution and updated every 6 hours. The modeled u and v component wind and temperature in atmosphere above the planetary boundary layer are nudged towards the NCEP Final reanalysis data with a 6-hour timescale (Stauffer and Seaman, 1990). In this way, the simulated key meteorological fields (e.g., surface temperature, precipitation, surface net solar radiation, and soil moisture) are close to the FNL reanalysis data (Fig. S2-S5 in the supporting material), which sets the base for further investigating the impacts of different MEGAN versions. There are a few days in July when the simulated surface solar radiation fluxes have positive biases, which may be due to the biases of clouds and the ignorance of aerosol radiative impacts in the simulations. The nudged simulations also guarantee that the difference in simulated BVOCs is from the difference in MEGAN versions instead of the meteorological difference.

Anthropogenic emissions for these simulations are obtained from the Hemispheric Transport of Air Pollution version-2 (HTAPv2) at 0.1°×0.1° horizontal resolution and monthly temporal resolution for 2010 (Janssens-Maenhout et al., 2015), while the

Multi-resolutions Emission Inventory for China (MEIC) at  $0.1^{\circ} \times 0.1^{\circ}$  horizontal resolution for 2015 (Li et al., 2017b; Li et al., 2017c) is used to replace the emissions over China within the simulation domain. Biomass burning emissions are obtained from the Fire Inventory from NCAR (FINN) at 1 km horizontal resolution and hourly temporal resolution (Wiedinmyer et al., 2011) and follow the injection heights proposed by Dentener et al. (2006) in the Aerosol Comparison between Observations and Models (AeroCom) and the diurnal variation provided by WRAP (2005). The GOCART dust emission scheme (Ginoux et al., 2001) is used to calculate the vertical dust flux, and the dust particles emitted into atmosphere are distributed by the MOSAIC aerosol size bins based on the physics of scale-invariant fragmentation of brittle materials provided by Kok (2011). Sea-salt emissions are similar to Zhao et al. (2013a), which corrected particles with radius less than  $0.2 \mu\text{m}$  and considered the dependence of the temperature of sea surface. More detailed details about the sea-salt emissions and dust emission scheme coupled with MOSAIC aerosol scheme in WRF-Chem can be found in (Zhao et al., 2010). Soil and lightning  $\text{NO}_x$  sources are not included in this study.

In order to investigate the sensitivities of simulated biogenic isoprene emissions by different versions of MEGAN to different vegetation distributions, as mentioned above, multiple experiments are conducted with different vegetation datasets and MEGAN versions, as summarized in Table 23. First of all, three experiments are conducted with the USGS vegetation distribution (VEG-USGS) using different versions of MEGAN embedded in WRF-Chem as discussed above, i.e., MEGANv1.0 (Mv1-USGS), MEGANv2.0 (Mv2-USGS), and MEGANv3.0 (Mv3-USGS). The sensitivities of biogenic emissions to different versions of MEGAN can be explored by comparing these three experiments. Second, another three experiments are conducted similar to the former ones but the VEG-USGS dataset is replaced by the VEG-2015 dataset, i.e., Mv1-2015, Mv2-2015, and Mv3-2015, respectively. By comparing these two sets of experiments, the impacts of the two vegetation distributions on the simulated BVOC emissions with each version of MEGAN can be investigated. These six experiments are conducted for both April and July. The seasonal variation of the sensitivities of BVOC emissions to different MEGAN versions and vegetation

distributions can be explored through the simulations for these two months.

### 3. Results

#### 3.1 Biogenic isoprene emission

##### 3.1.1 Sensitivity to emission schemes and vegetation distributions

Figure 3 shows the spatial distributions of biogenic isoprene emission averaged in April for six simulations with different vegetation datasets and biogenic emission schemes. First of all, with the same vegetation dataset of USGS, ~~the large difference exists~~<sup>differences exist</sup> among the results from these three versions of emission scheme. In terms of domain average, MEGANv2.0 simulates the highest isoprene emission among the three versions, MEGANv3.0 follows, and MEGANv1.0 simulates the lowest, especially over the northwest of the simulation domain. It can also be noticed that the spatial distributions of biogenic isoprene emission are different among the versions. To illustrate better the difference, two focused areas (denoted by the red and black boxes in Fig. 3) in the simulation domain are selected for further analysis. Over the southwest region of domain (denoted by the black box), the averaged biogenic isoprene emission in Mv1-USGS is below 0.2 mole/km<sup>2</sup>/hr, and it is about 1.0 mole/ km<sup>2</sup>/hr and 3.1 mole/km<sup>2</sup>/hr from the Mv3-USGS and Mv2-USGS simulations, respectively. Over the southeast region of domain (denoted by the red box), similarly, the MEGANv2.0 simulates the highest biogenic isoprene emission among the three versions and MEGAN v1.0 estimates more emissions than MEGAN v3.0.

Over the southwest region of domain, for MEGAN v1.0, irrigated cropland (the 3rd land use type in VEG-USGS), cropland with grassland mosaic (the 5th), and savanna (the 10th) are the dominant land use types over the southwest region (Fig. 1), which have low emission factors (as shown in Fig. 2). For MEGAN v3.0, crop and grass are the dominant PFTs over the region, but some temperate needle-leaf evergreen trees that have higher emission factor of about 3 mg isoprene/m<sup>2</sup>/hr (as shown in Fig. 32) are also included in this area (Fig. 1). The different vegetation distributions lead to the overall emission factors are different between MEGANv1.0 and



MEGANv2/MEGANv3.0 (Fig. 4). Therefore, MEGAN v3.0 simulated more biogenic isoprene emissions than MEGAN v1.0 (0.88 mole/km<sup>2</sup>/hr versus 0.42 mole/km<sup>2</sup>/hr) over this region. Over the southeast region of domain, the dominant land use type is cropland with woodland mosaic (the 6<sup>th</sup>) that has high emission factor of about 2 mg isoprene/m<sup>2</sup>/hr and irrigated cropland in MEGAN v1.0. By contrast, the PFTs in MEGAN v3.0 is crop and has lower emission factor. This leads to larger overall emission factor in MEGANv1.0 than in MEGANv3.0 over this region. Therefore, MEGANv1.0 calculates more biogenic isoprene emissions than MEGANv3.0 (1.08 mole/km<sup>2</sup>/hr versus 0.65 mole/km<sup>2</sup>/hr) over the area. In general, the difference between MEGANv1.0 and MEGANv3.0 with the same USGS land-use dataset is mainly due to the conversion of the USGS land-use to PFT that leads to different vegetation types with different emission factors in each grid. For MEGANv2.0, the emission factor of isoprene is obtained from the input database directly in WRF-Chem, and it is the highest among the three versions of MEGAN (Fig. 4). Therefore, MEGANv2.0 simulates the most biogenic isoprene emissions over the two analyzed regions among the three different versions independent of the vegetation coverage (will be discussed below).

In terms of the modeling sensitivities to vegetation distributions (i.e., VEG-USGS versus VEG-2015), as discussed above, with prescribed emission factor of isoprene at each grid cell, the isoprene emission from MEGANv2.0 in WRF-Chem does not change much with different vegetation distributions except some small perturbation due to the impacts of vegetation distributions on meteorological fields. Over the southwest of domain, the averaged biogenic isoprene emission with VEG-2015 is higher (0.68 mole/km<sup>2</sup>/hr and 2.25 mole/km<sup>2</sup>/hr) than that (0.42 mole/km<sup>2</sup>/hr and 0.88 mole/km<sup>2</sup>/hr) with VEG-USGS for both MEGANv1.0 and MEGANv3.0 due to the increased fraction of needle-leaf evergreen tree and mixed forest over this area (Fig. 1) in VEG-2015, and these land use types have higher emission factors (Fig. 2) than croplands in VEG-USGS. Over the southeast, the vegetation coverage is significantly reduced from VEG-2015 to VEG-USGS due to the rapid development in economic and urban expansion over the region in last two decades. Therefore, for MEGANv1.0, the averaged isoprene emission from Mv1-2015 is lower (0.39 mole/km<sup>2</sup>/hr) than that

(1.08 mole/km<sup>2</sup>/hr) from Mv1-USGS, consistent with the lower overall emission factor with VEG-2015 compared to VEG-USGS in MEGANv1.0 (Fig. 4). However, it is noteworthy that, for MEGANv3.0, the isoprene emission from Mv3-2015 is higher (1.12 mole/km<sup>2</sup>/hr) than that (0.65 mole/km<sup>2</sup>/hr) from Mv3-USGS. The different sensitivities of the two versions to the vegetation changes are mainly due to their different treatments of sub-grid vegetation distribution as discussed in Sect. 2.2, i.e., MEGANv3.0 considers sub-grid vegetation distribution besides the dominant vegetation type at each grid cell when ~~estimate~~[estimating](#) the BVOCs emissions, while MEGANv1.0 only considers the dominant vegetation type at each grid cell.

To further demonstrate the impact of sub-grid distribution of vegetation in MEGANv3.0, Figure 5 shows the difference of major sub-grid fraction of PFT other than the dominant one over the southeast region of domain within the red box between VEG-2015 and VEG-USGS. Although the dominant vegetation types are crops, grass, and bare soil over the region (Fig. 1), the sub-grid fractions of needle-leaf evergreen tree, broad-leaf evergreen tree, and broad-leaf deciduous tree that have relatively higher emission factors (Fig. 2) are higher in VEG-2015 than in VEG-USGS. As shown in Fig. 4, the overall emission factor  $\varepsilon_{i,j}$  weighted by sub-grid PFT fractions is higher with VEG-2015 than with VEG-USGS from MEGANv3.0. It highlights that the sub-grid vegetation distribution is important in terms of estimating BVOC emissions over this region, which results in more biogenic isoprene emission in MEGANv3.0 than MEGANv1.0 with the latest vegetation distribution dataset (i.e., VEG-2015).

### 3.1.2 Environmental impacts

Besides emission factor, biogenic emission is also influenced by activity factor that is largely controlled by environmental conditions. The activity factor mainly accounts for the response of biogenic emission to temperature, leaf age, soil moisture, solar radiation, leaf area index, and drought in ~~current~~[the three](#) versions of MEGAN [in WRF-Chem](#). The seasonal variations (July versus April) of simulated biogenic emissions by different versions of MEGAN with VEG-2015 are investigated to demonstrate the environmental impacts and their difference among MEGAN versions.

Please note that emission factors are not dependent on seasons. Figure 6 shows the ratios of monthly averaged biogenic isoprene emission and overall activity factor ( $\gamma_i$ ) between July and April from three versions of MEGAN with the VEG-2015 vegetation dataset. Only the simulation results with VEG-2015 are analyzed here due to the similar results with VEG-USGS (not shown). It is evident that the ratios are all greater than one, which means much more isoprene is emitted into atmosphere by plant in July than in April. The seasonal variations of magnitudes and the distributions of activity factors are consistent with those of emissions. Among different versions, MEGANv3.0 is most sensitive to environmental conditions, especially over the north of domain between 32°N and 36°N.

The overall activity factor is the product of the factors determined by temperature, LAI, solar radiation, leaf age, and drought condition in MEGANv2.0 and MEGANv3.0 while it is an overall function of temperature and solar radiation in MEGANv1.0 that cannot be separated as isolated factors. Therefore, for MEGAN v2.0 and MEGAN v3.0, the ratios of isolated activity factors responding to temperature, LAI, solar radiation, leaf age, and drought between July and April are further illustrated in Figure 7. The temperature-dependent activity factor ( $\gamma_t$ ) plays an important role in the seasonal change of total activity factor, especially in the north of simulation domain, which is about 3.0~4.0 and >4.0 in MEGANv2.0 and MEGANv3.0, respectively, which means that MEGAN predicts higher biogenic isoprene emission in warmer environment. Guenther (2006) also point that the temperature-dependent activity factor increases evidently with temperature.

There are two activity factors associated with leaves. One is related to the emission dependence of absolute values of LAI ( $\gamma_{LAI}$ ), which has the most different distributions among all activity factors in two versions. The ratio in MEGAN v3.0 is above 4 and < 2 in MEGAN v2.0 over the most part of simulation domain. It is noteworthy that the ratio is below 1 in MEGAN v2.0 in the north of the domain while it is more than 4 in MEGAN v3.0, that dominant the difference between July and April. Figure 8 shows the change of activity factor for LAI as a function of LAI value used in MEGAN v2.0 and MEGAN v3.0, respectively. It is evident that the estimated LAI

activity factors in both versions increase with the LAI values, but with different increasing rates. In general, MEGANv3.0 has the faster increasing rate. Please note, as discussed previously in Sect. 2.2, MEGAN v3.0 obtains the LAI online from the land surface scheme directly that can capture the seasonal change well, while MEGAN v2.0 obtains it from climatological monthly mean input dataset that is different from the one used in the land surface scheme in WRF-Chem. Figure 9 shows the distributions of LAI in MEGAN v2.0 and MEGAN v3.0 in different months. For MEGAN v2.0, LAI has almost no change from April to July, particularly over the northern simulation domain, while for MEGAN v3.0, the LAI increases evidently over the whole domain, especially over the north. Therefore, the ratio of  $\gamma_{LAI}$  between July and April is around one in MEGANv2.0, while it is much larger than one in MEGANv3.0.

The second is related to the leaf age ( $\gamma_a$ ) that also has quite different distributions between MEGANv2.0 and MEGANv3.0. For MEGAN v2.0, the ratio is about 1~3 in the most area while it below 1.0 between 30°N and 34°N, and more than 2 in the northwest of simulation domain. For MEGAN v3.0, the ratio is above 1.0 over the whole domain and the distribution has significant regional difference. It is 1~1.3 in the south region while more than 2 in the north region. Generally speaking, leaf's ability to emit biogenic isoprene is significantly influenced by leaf phenology. Young leaves emit almost no isoprene, mature leaves emit mostly, and old leaves lose ability to produce biogenic isoprene eventually. ([Guenther et al., 2006](#)). Therefore, plants emit more isoprene into atmosphere in July than in April because of more mature leaves due to the plant growth. Activity factor for leaf age is a function of the relative change of emission activity and the fraction of leaves at different phenological stages that are determined by the difference of LAI in current and previous month, [introduced by Jiang et al. \(2018\)](#). In both versions of MEGAN, mature and old foliage have highest relative isoprene emission activity, following by the growing foliage and the new foliage is the lowest. Therefore, MEGAN v3.0 produce higher leaf age activity factor in July because of the larger difference of LAI in different month and more mature foliage to emit isoprene (Fig. 9).

The distribution of the ratio of light-~~depend~~[dependent](#) activity factor ( $\gamma_p$ ) is also

different between the two versions. Light-~~depend~~dependent activity factor ( $\gamma_P$ ) is a function of PPFD and activity of isoprene synthase, and is dominated by the variation of PPFD. In general, plants often have higher light-~~depend~~dependent activity factor in July than that in April due to the stronger radiation. For MEGAN v2.0, it is about 1~1.5 over the whole domain and has no significant regional difference. For MEGAN v3.0, the ratio is below 1 in the south of the domain while it is about 1.3~1.5 or more than 2 in the north of the domain. MEGAN v3.0 considered the difference of sunlit and shaded leaves and PPFD will be low on shaded leaves in dense canopy because of the blocking sunlight. Therefore, MEGAN v3.0 calculated low light-depend activity factor in the south of the domain due to the distribution of mixed forest which has dense canopy in summer.

The seasonal variation of drought-dependent activity factor ( $\gamma_{d,isoprene}$ ) is only included in MEGANv3.0 with the ratios of 1~3 over the domain. Previous studies have shown that plants emit more isoprene into atmosphere under short-term mild drought stress (e.g., Jiang et al., 2018). The reduction of stomatal conductance is accompanied with the increase in leaf temperature resulting in the more isoprene emissions from plants (Jiang et al., 2018). As mentioned in the methodology, the empirical coefficient  $\alpha$  of 37 is applied for drought activity factor calculation following Jiang et al. (2018) in this study due to the lack of observation and experiment constraint over China. To examine its potential effect on calculating drought activity factor in China, sensitivity experiments are conducted with different values of  $\alpha$ . The results indicate that the value of  $\alpha$  has small effect on the seasonal variation and the spatial distribution of drought activity factor over East China (Fig. S6 in the supporting material), which is consistent with Jiang et al. (2018) that also stated the drought effect on seasonal change of isoprene emissions in China was not evident. In addition, as discussed in the Section 2.2, drought-dependent activity factor is proportional to photosynthetic enzyme activity, which can be affected by PPFD. Therefore, MEGAN v3.0 estimated more isoprene emissions in July especially in the north of domain and the pattern is similar to the distribution of light-depend activity factor.

### 3.1.3 Comparison with observations

The results discussed above show the difference in modeling biogenic emissions of isoprene. The difference of simulated near-surface isoprene concentrations is similar as their emissions (not shown here). It will be optimal to compare the simulated isoprene emissions and concentrations from different experiments with observations. However, as far as we know, the publicly available in-situ measurements of isoprene emissions and concentrations over East China is extremely sparse. ~~Meanwhile, although the satellite retrieved column integrated formaldehyde is often used for evaluating simulated BVOCs, it is not suitable for using in this study because the production from anthropogenic VOCs dominates the column formaldehyde over most regions of East China. It is difficult to isolate the contribution from BVOCs to formaldehyde from satellite retrievals. Since it is difficult to evaluate the simulated results over a large area of East China, the limited observations are~~Only limited observations can be collected from published literatures and unpublished data over both rural and urban areas of East China ~~to compare~~for comparison with the results of different experiments as listed in Table 34.

In general, the simulated ~~results with~~isoprene concentrations from MEGANv2.0 and MEGANv3.0 are closer to measurements: ~~in these four sites listed in Table 4 while~~ MEGANv1.0 generally underestimates the observed values. ~~Although Compared with the results from MEGANv2.0 and MEGANv3.0 are quite different in some cases, they are both within the uncertain range of limited observations in general. Although, as,~~ MEGANv2.0 produces higher isoprene concentrations in most sampling sites except the site of Lishui-District surrounded with the densely vegetation-covered suburb. As discussed above, MEGANv3.0 can ~~capture the~~simulate higher biogenic isoprene emissions in urban area due to its consideration of sub-grid vegetation distributions, ~~it is difficult to be evaluated with these limited data, except that at one site~~At the sampling sites in urban area, such as the sites of Xujiahui, Shanghai, and Nanjing, the simulation with MEGANv3.0 produces higher surface concentration of isoprene ~~that is closer to the observation~~compared to that with MEGANv1.0. In MEGANv2.0, the prescribed vegetation distributions do not reflect the urbanization over East China. Therefore, the

621 simulated isoprene concentrations between these two versions are comparable. Overall,  
622 the experiments with MEGANv2.0 and MEGANv3.0 may simulate better surface  
623 concentration of isoprene over East China than that with MEGANv1.0, ~~and more high-~~  
624 ~~quality observations of BVOCs concentrations in both rural and urban areas of East~~  
625 ~~China are definitely needed to further validate the modeling results in future.~~ Please  
626 note that these observations were collected at different sites for different periods. Ideally,  
627 the observations at multiple sites or from aircraft for a specific period are needed to  
628 evaluate overall model performance of BVOCs over a region (e.g., Zhao et al., 2016).  
629 It is difficult to evaluate effectively any simulations with those observations listed in  
630 Table 4.

631 Besides in-situ and aircraft measurements, satellite retrieved column integrated  
632 formaldehyde is often used for evaluating modeling results of VOCs over a large area.  
633 Tropospheric formaldehyde vertical column concentrations have been retrieved from  
634 the Ozone Mapping and Profiler Suite (OMPS) (Abad et al., 2016), which is one of the  
635 instruments onboard the Suomi National Polar-orbiting Partnership (Suomi-NPP). The  
636 satellite flies on a sun-synchronous polar orbit with daily global coverage and  
637 measurements are combined into 35 cross-track bins giving a spatial resolution of 50  
638 km×50 km. It crosses the equator around 13:30 local solar time in the ascending mode.  
639 (Su et al. 2019, Su et al. 2020). Figure 10 shows the monthly mean total tropospheric  
640 column concentration of formaldehyde from the satellite retrievals and the simulations  
641 with different versions of MEGAN in April and July. In general, the simulated  
642 tropospheric column concentrations of formaldehyde are consistent with satellite  
643 retrievals in April, showing high column formaldehyde concentration over the Yangtze  
644 River Delta region and South China. The formaldehyde concentrations are contributed  
645 comparably by both anthropogenic and biogenic sources over these two regions, and  
646 the biogenic source contributes about 20% to the total in April (Fig. S7 in the supporting  
647 material). Although there are some small differences in formaldehyde column  
648 concentrations in April among the simulations with different MEGAN versions,  
649 consistent with the comparison of biogenic emissions (Fig. 3), it is difficult to apply the  
650 satellite retrievals to constrain their small difference if considering the uncertainties of

retrievals. In July, the difference among the simulations with different MEGAN versions is much larger. Compared to the satellite retrievals, the simulation with MEGANv1.0 (MEGANv3.0) may underestimate (overestimate) tropospheric formaldehyde column concentrations. These biases may reflect their errors in biogenic emissions. The large difference between MEGANv2.0 and MEGANv3.0 in July may indicate that some activity factors controlling seasonal variation of BVOCs emissions is less appropriate in MEGANv3.0 than in MEGANv2.0. However, please note that satellite retrievals of formaldehyde may also have relatively large uncertainties in July (e.g., Su et al., 2019; Su et al., 2020) and the uncertainties of anthropogenic emissions of VOCs may also contribute to the modeling biases of formaldehyde.

Through the sensitivity analysis and comparison with satellite retrievals, activity factors corresponding to temperature and LAI are most important for seasonal variation of BVOCs. The different functions of activity factor for LAI in MEGANv2.0 and MEGANv3.0 need to be constrained with observations. The empirical coefficient for calculating drought activity factor also need to be constrained for China with more laboratory and field experiments. Therefore, high-quality direct observations of BVOCs emissions or concentrations for different season at multiple sites or from aircrafts in both rural and urban areas of East China are definitely needed to evaluate overall model performance of BVOCs over the region. Satellite retrieval of formaldehyde alone is still difficult to constrain uncertain parameters or functions in BVOCs emission scheme, particularly over the regions like China. The modeling sensitivity analysis also suggests some specific areas, such as the Anhui and Henan provinces in the north of domain, that particularly need more reliable observations of BVOCs to constrain the large modeling sensitivities.

### 3.2 Impacts on mixing ratio of VOCs and ozone

Difference in emissions of BVOCs from multiple versions of MEGAN can influence the simulated mixing ratio of VOCs over East China that can further significantly affect ozone production through photochemistry (Wei et al., 2007; Bao et al., 2010; Calfapietra et al., 2013; Kim et al., 2013; Liu et al., 2018; Lu et al., 2019).

带格式的: 缩进: 首行缩进: 0 字符



The photochemistry is most active in summer, therefore, the simulation results in July with the latest vegetation coverage (VEG-2015) are analyzed here. Figure 4011 shows the distributions of total VOCs and HCHO concentrations near the surface contributed by the BVOCs emissions simulated by the model with different versions of MEGAN using VEG-2015 in July. [The concentrations of species contributed by biogenic emissions are estimated through calculating the difference between the control simulation and the simulation without biogenic emissions.](#) It is evident that BVOCs contribute significantly, [25% and 35% on average](#), to the amount of total VOCs [and formaldehyde, respectively](#), over East China, and the difference among the simulations with the three versions of MEGAN is large. [\(Fig. S8 in the supporting material\)](#). The simulation with MEGANv3.0 produces the highest biogenic VOCs concentration (> 20 ppb), followed by MEGANv2.0 (10-20 ppb), and the one with MEGAN v1.0 is the lowest (< 5 ppb), particularly over the northern region. In terms of spatial distribution, the simulation with MEGANv3.0 generates higher biogenic VOCs concentration over the north of domain, while the ones with the other two versions of MEGAN generate higher concentration over the south, which is consistent with the spatial distributions of the total biogenic emissions simulated by different MEGAN versions in WRF-Chem [\(Fig. S4S9 in the supporting material\)](#). The spatial distributions of simulated biogenic contribution to the surface formaldehyde concentration are consistent with those of biogenic VOCs.

The significantly increased amounts of biogenic VOCs may induce the increase of surface ozone concentration over East China (Zhao et al., 2009). Figure 4112 demonstrates the spatial distribution of monthly mean ozone mixing ratio near the surface contributed by the emissions of BVOCs. The simulation with MEGANv3.0 produces the largest amount of biogenic ozone over a large area of the simulation domain. The biogenic ozone from the simulation with MEGANv3.0 is estimated over 8 ppb while it is 2~5 ppb from the one with MEGAN v2.0 and less than 1 ppb from the one with MEGANv1.0. For MEGANv1.0 and MEGAN v3.0, the distributions of surface biogenic ozone concentration is consistent with those of biogenic VOCs, for example, MEGAN v3.0 estimated more biogenic VOCs over the north of the domain

while ozone concentration is also simulated higher in the same region. For MEGAN v2.0, it is evident that the ozone formation is not influenced by biogenic VOCs solely. The ozone production can be determined by the changes of both VOCs and NO<sub>x</sub> concentrations, and the production efficiency can be different for NO<sub>x</sub>-sensitive region and VOCs-sensitive region (e.g., Zhao et al., 2009).

Figure 4213 shows the surface concentrations of NO<sub>x</sub> due to the biogenic emissions simulated with three versions of MEGAN with VEG-2015. The results are calculated as the difference between simulations with and without biogenic emissions. The simulations with MEGANv3.0 estimate the highest BVOCs-contributed concentration change, especially over the north of domain (>2 ppb), followed by MEGAN v2.0 (0.2-0.4ppb), and MEGAN v1.0 simulated lowest concentration (about 0.1ppb and below 0). The different changes of surface NO<sub>x</sub> concentrations are mainly caused by the different impacts on NO<sub>x</sub> lifetime due to biogenic VOCs. The increase of surface NO<sub>x</sub> concentration is due to the BVOC-induced increase of NO<sub>x</sub> lifetime reflected by the reduction of surface OH concentration (Fig. S2S10 in the supporting material). Therefore, the increase of ozone contributed by biogenic emissions in the north of the domain (30°N-36°N) simulated with MEGANv2.0 is due to the combined effect of increased NO<sub>x</sub> and VOCs surface concentrations. It is also noteworthy that the surface ozone concentrations are simulated lower over the southeast of domain than that in the southwest with the three versions of MEGAN, while the surface concentrations of BVOCs have no significant difference between the two regions. This is mainly due to that the southwest is more sensitive to VOCs in terms of ozone production (Fig. S3S11 in the supporting material) (e.g., Zhao et al., 2009).

#### 4. Summary and conclusion

In this study, three versions of MEGAN in WRF-Chem and their difference in simulating BVOC emissions and impacts on ozone mixing ratio over East China is documented in the literature for the first time. The latest version of MEGAN v3.0 is coupled within CLM4 land scheme as a part of WRF-Chem. Specifically, MEGAN v3.0

is updated from MEGAN v2.1 as an option in biogenic emission schemes and can share the consistent vegetation map and other variables with CLM4 such as surface temperature and leaf area index. What's more, MEGAN v3.0 ~~include~~includes the activity factor for drought and the combination of different versions of MEGAN and CLM4 are employed to investigate the sensitivity of the variation of MEGAN versions. Experiments are conducted for April and July over Eastern China with VEG-USGS and VEG-2015 to study the sensitivities of simulated BVOCs by different MEGAN versions in WRF-Chem to seasonal change and the distributions of vegetation. The main conclusions are summarized below.

Physical and ~~chemistry~~chemical processes in these three versions of MEGAN implemented in WRF-Chem are different, and the most intuitive distinction is their different treatments of emission factor of BVOCs. MEGANv1.0 prescribed constant values for different land use categories at each grid cell, and MEGANv2.0 has a stand-alone PFT specific emission factor map. For MEGAN v3.0, the overall emission factor at each grid cell is calculated by PFT-specific emission factor and the fraction of each PFT. Therefore, the biogenic isoprene emissions estimated by three versions of MEGAN are different over the simulation domain. The VEG-USGS and VEG-2015 datasets present quite different distributions of vegetation coverage, which also contributes to the difference of emission factors among different versions. Different versions of MEGAN show different sensitivities to the changes of vegetation distributions due to their different treatments of vegetation fraction in estimating emission factors of BVOCs. The results highlight the importance of considering sub-grid vegetation fraction in estimating BVOCs emissions. MEGANv3.0 with sub-grid vegetation distribution simulates higher BVOCs emissions over the urban area of the Yangtze River Delta (YRD) region compared to MEGANv2.0 with only the dominant vegetation type at each grid cell.

Activity factor plays an important role in determining the seasonal change of BVOCs emissions. Simulations with different versions of MEGAN show different seasonal variation of activity factors and thus BVOCs emissions. The results indicated that overall activity factor in July is higher than the one in April in all versions of

MEGAN, and MEGAN v3.0 is most sensitive to the seasonal change especially in the north of simulation domain. In general, among all activity factors, temperature-dependent factor dominates the seasonal change of activity factor in all three versions of MEGAN, while the different response to the LAI change determines the difference among the three versions in seasonal variation of BVOC emissions. The additional drought-dependent activity factor in MEGANv3.0 can result in a little higher BVOC emission over East China in July than April due to the increasing photosynthetic enzyme activity, i.e., plants emit more biogenic isoprene in July than that in April under the short-term mild drought forcing. The overall drought impact on BVOC emissions over East China is small as previous studies (e.g., Jiang et al., 2018).

Different BVOCs simulated with the three versions of MEGAN in WRF-Chem lead to the large difference in ozone production. The simulation with MEGANv3.0 produces the highest BVOCs contributed ozone concentration ( $> 8$  ppbv) over East China among the three versions, followed by the simulations with MEGANv2.0 and MEGAN v1.0. The difference of BVOCs contributed ozone among the simulations with three versions of MEGAN is not only affected by the increased concentration of BVOCs but also influenced by the changes of NO<sub>x</sub> concentration. The simulations with different versions of MEGAN show different distributions of surface NO<sub>x</sub> concentration due to the BVOCs-induced changes of NO<sub>x</sub> lifetime. The production efficiency of surface ozone concentration over East China due to BVOCs also depends on the regions as NO<sub>x</sub>-sensitive or VOCs-sensitive regions.

Although the analysis in this study is for one single year, the investigation of simulations for a different year demonstrates similar results (not shown), which indicate the modeling sensitivities with different versions of MEGAN do not change significantly with years. This study highlights that the simulated emissions of BVOC over East China is sensitive to vegetation coverage, which has also been found by previous studies (e.g., Klinger et al., 2002; Wang et al., 2007). However, this study further demonstrates that the modeling sensitivity to vegetation coverage could be quite different depending on the BVOC emission schemes. Some studies also showed that BVOC emissions can be more than 50% higher in summer than in other seasons (e.g.,

带格式的: 缩进: 首行缩进: 2 字符

Li et al., 2020), which may be also sensitive to the formulas of emission activity factors in different emission algorithms as discussed in this study. Large ~~uncertainties in~~ modeling ~~sensitivities in simulating~~ BVOCs emission over East China still exist as reflected by different versions of the ~~scheme~~MEGAN, consistent with previous studies that found the off-line calculation with different versions of MEGAN led to significantly different BVOC emissions over China. Although it is evident that surface ozone concentration can be significantly influenced by BVOC emissions over East China through affecting VOCs, OH, and NO<sub>x</sub> and the BVOC impact is also region-sensitive as found in this and previous works (e.g., Geng et al., 2011; Tie et al., 2013; Liu et al., 2018), this study highlights that the overall impact can be quite sensitive to different algorithms in ~~emission schemes~~different MEGAN version.

~~Due to these large uncertainties in emission factor, activity factor,~~Theoretically, MEGANv3.0 that is coupled with the land surface scheme and considers the sub-grid vegetation ~~distribution in estimating BVOC~~effect should overcome previous versions of MEGAN in WRF-Chem, however, considering uncertainties of retrievals and anthropogenic emissions over East China, ~~the limited in-situ~~ observations ~~of BVOC species such isoprene and monoterpene~~or satellite retrieval of formaldehyde alone is still difficult to constrain uncertain parameters or functions in BVOCs emission schemes applied over East China. High-quality direct observations of BVOCs emissions or concentrations for different season at multiple sites or from aircrafts in both rural and urban areas of East China are ~~urgently~~definitely needed to evaluate ~~the overall~~ model and then further quantify performance of BVOCs over China, particularly over some specific areas with large modeling sensitivities of BVOC emission and activity factors, such as the ~~impacts of BVOCs on ozone and organic aerosols~~.Anhui and Henan provinces in the north of simulation domain, suggested by this study. In addition, direct measurements of biogenic emission fluxes and/or emission factors and activity factors ~~are needed in the laboratory may be also helpful~~ to constrain different ~~emission algorithm~~activity factor functions of MEGAN in atmospheric models. ~~Last~~Lastly but not the least, ~~the~~Although, theoretically, VEG-2015 should be more representative for the reality in 2015, particularly for East China with intensive

带格式的: 缩进: 首行缩进: 0 字符

urban expansion since 2000s, it could still have some uncertainties, particularly for the specification of various vegetation types. The survey of more accurate and higher resolution vegetation distribution based on in-situ survey and investigation and satellite remote sensing should be conducted to support the estimation of BVOC emission over East China.

### Data availability

The released version of WRF-Chem can be downloaded from [http://www2.mmm.ucar.edu/wrf/users/download/get\\_source.html](http://www2.mmm.ucar.edu/wrf/users/download/get_source.html). The code of updated USTC version of WRF-Chem can be downloaded from <http://aemol.ustc.edu.cn/product/list/https://doi.org/10.5281/zenodo.4663508> or contact chunzhao@ustc.edu.cn. Also, the code modifications will be incorporated the release version of WRF-Chem in future.

### Author contributions

Mingshuai Zhang and Chun Zhao designed the experiments, conducted and analyzed the simulations. All authors contributed to the discussion and final version of the paper.

### Acknowledgements

This research was supported by the Fundamental Research Funds for the Central Universities, and the National Natural Science Foundation of China (grant 41775146), the USTC Research Funds of the Double First-Class Initiative, and the Strategic Priority Research Program of Chinese Academy of Sciences (grant XDB41000000). The study used the computing resources from the High-Performance Computing Center of University of Science and Technology of China (USTC) and the TH-2 of National Supercomputer Center in Guangzhou (NSCC-GZ).

861  
862  
863  
864

865

## Reference

- Abdi-Oskouei, M., Pfister, G., Flocke, F., Sobhani, N., Saide, P., Fried, A., Richter, D., Weibring, P., Walega, J., and Carmichael, G.: Impacts of physical parameterization on prediction of ethane concentrations for oil and gas emissions in WRF Chem, *Atmos. Chem. Phys.*, 18, 16863–16883, 2018.
- Arghavani, S., Malakooti, H., and Bidokhti, A. A.: Numerical evaluation of urban green space scenarios effects on gaseous air pollutants in Tehran Metropolis based on WRF Chem model, *Atmospheric Environment*, 214, 116832, 2019.
- Arneth, A., Niinemets, Ü., Pressley, S., Bäck, J., Hari, P., Karl, T., Noe, S., Prentice, I. C., Serça, D., Hickler, T., Wolf, A., and Smith, B.: Process-based estimates of terrestrial ecosystem isoprene emissions: incorporating the effects of a direct CO<sub>2</sub>-isoprene interaction, *Atmos. Chem. Phys.*, 7, 31–53, 2007.
- Bao, H., Shrestha, K. L., Kondo, A., Kaga, A., and Inoue, Y.: Modeling the influence of biogenic volatile organic compound emissions on ozone concentration during summer season in the Kinki region of Japan, *Atmospheric Environment*, 44, 421–431, 2010.
- Bonan, G. B.: Land surface model (LSM version 1.0) for ecological, hydrological, and atmospheric studies: Technical description and user's guide. Technical note, United States, 1996.
- Brown, S. S., Dubé, W. P., Bahreini, R., Middlebrook, A. M., Broek, C. A., Warneke, C., de Gouw, J. A., Washenfelder, R. A., Atlas, E., Peisehl, J., Ryerson, T. B., Holloway, J. S., Schwarz, J. P., Spackman, R., Trainer, M., Parrish, D. D., Fehsenfeld, F. C., and Ravishankara, A. R.: Biogenic VOC oxidation and organic aerosol formation in an urban nocturnal boundary layer: aircraft vertical profiles in Houston, TX, *Atmos. Chem. Phys.*, 13, 11317–11337, 2013.
- Calfapietra, C., Fares, S., Manes, F., Morani, A., Sgrigna, G., and Loreto, F.: Role of Biogenic Volatile Organic Compounds (BVOC) emitted by urban trees on ozone concentration in cities: A review, *Environmental Pollution*, 183, 71–80, 2013.
- Carlton, A. G., Wiedinmyer, C., and Kroll, J. H.: A review of Secondary Organic Aerosol (SOA) formation from isoprene, *Atmos. Chem. Phys.*, 9, 4987–5005, 2009.
- Carslaw, N., Bell, N., Lewis, A. C., McQuaid, J. B., and Pilling, M. J.: A detailed case study of isoprene chemistry during the EASE96 Mace Head campaign, *Atmospheric Environment*, 34, 2827–2836, 2000.
- Dentener, F., Kinne, S., Bond, T., Boucher, O., Cofala, J., Generoso, S., Ginoux, P., Gong, S., Hoelzemann, J. J., Ito, A., Marelli, L., Penner, J. E., Putaud, J. P., Textor, C., Schulz, M., van der Werf, G. R., and Wilson, J.: Emissions of primary aerosol and precursor gases in the years 2000 and 1750 prescribed data sets for AeroCom, *Atmos. Chem. Phys.*, 6, 4321–4344, 2006.
- Derognat, C., Beekmann, M., Bacumle, M., Martin, D., and Schmidt, H.: Effect of biogenic volatile organic compound emissions on tropospheric chemistry during the Atmospheric Pollution Over the Paris Area (ESQUIF) campaign in the Ile-de-France region, *J. Geophys. Res. Atmos.*, 108, 15, 2003.
- Fast, J. D., Gustafson Jr, W. I., Easter, R. C., Zaveri, R. A., Barnard, J. C., Chapman, E.



G., Grell, G. A., and Peckham, S. E.: Evolution of ozone, particulates, and aerosol direct radiative forcing in the vicinity of Houston using a fully coupled meteorology chemistry aerosol model, *Journal of Geophysical Research: Atmospheres*, 111, 2006.

Forkel, R., Balzarini, A., Baró, R., Bianconi, R., Curci, G., Jiménez-Guerrero, P., Hirtl, M., Honzak, L., Lorenz, C., Im, U., Pérez, J. L., Pirovano, G., San José, R., Tuccella, P., Werhahn, J., and Žabkar, R.: Analysis of the WRF Chem contributions to AQMEII phase2 with respect to aerosol radiative feedbacks on meteorology and pollutant distributions, *Atmospheric Environment*, 115, 630–645, 2015.

Friedl, M. A., McIver, D. K., Hodges, J. C. F., Zhang, X. Y., Muchoney, D., Strahler, A. H., Woodcock, C. E., Gopal, S., Schneider, A., Cooper, A., Baccini, A., Gao, F., and Schaaf, C.: Global land cover mapping from MODIS: algorithms and early results, *Remote Sensing of Environment*, 83, 287–302, 2002.

Fu, P., Kawamura, K., Kanaya, Y., and Wang, Z.: Contributions of biogenic volatile organic compounds to the formation of secondary organic aerosols over Mt. Tai, Central East China, *Atmospheric Environment*, 44, 4817–4826, 2010.

Geng, F., Tie, X., Guenther, A., Li, G., Cao, J., and Harley, P.: Effect of isoprene emissions from major forests on ozone formation in the city of Shanghai, China, *Atmos. Chem. Phys.*, 11, 10449–10459, 2011.

Geron, C. D., Guenther, A. B., and Pierce, T. E.: An improved model for estimating emissions of volatile organic compounds from forests in the eastern United States, *Journal of Geophysical Research: Atmospheres*, 99, 12773–12791, 1994.

Ghude, S. D., Pfister, G. G., Jena, C., van der A, R. J., Emmons, L. K., and Kumar, R.: Satellite constraints of nitrogen oxide (NO<sub>x</sub>) emissions from India based on OMI observations and WRF Chem simulations, *Geophysical Research Letters*, 40, 423–428, 2013.

Ginoux, P., Chin, M., Tegen, I., Prospero, J. M., Holben, B., Dubovik, O., and Lin, S.-J.: Sources and distributions of dust aerosols simulated with the GOCART model, *Journal of Geophysical Research: Atmospheres*, 106, 20255–20273, 2001.

Gregorio, A.: Land Cover Classification System (LCCS), version 2: Classification Concepts and User Manual: LCCS, Number 8. Food & Agriculture Organization, Rome, Italy., FAO Environment and Natural Resources Service Series, 8, 2005.

Grell, G. A., Peckham, S. E., Schmitz, R., McKeen, S. A., Frost, G., Skamarock, W. C., and Eder, B.: Fully coupled “online” chemistry within the WRF model, *Atmospheric Environment*, 39, 6957–6975, 2005.

Guenther, A.: Biological and Chemical Diversity of Biogenic Volatile Organic Emissions into the Atmosphere, *ISRN Atmospheric Sciences*, 2013, 2013.

Guenther, A.: Estimates of global terrestrial isoprene emissions using MEGAN (Model of Emissions of Gases and Aerosols from Nature), *Atmos. Chem. Phys.*, 7, 4327–4327, 2006.

Guenther, A., Hewitt, C. N., Erickson, D., Fall, R., Geron, C., Graedel, T., Harley, P., Klinger, L., Lerdau, M., McKay, W. A., Pierce, T., Scholes, B., Steinbrecher, R., Tallamraju, R., Taylor, J., and Zimmerman, P.: A global model of natural volatile

organic compound emissions, *Journal of Geophysical Research: Atmospheres*, 100, 8873–8892, 1995.

Guenther, A., Zimmerman, P., Klinger, L., Greenberg, J., Ennis, C., Davis, K., Pollock, W., Westberg, H., Allwine, G., and Geron, C.: Estimates of regional natural volatile organic compound fluxes from enclosure and ambient measurements, *J. Geophys. Res. Atmos.*, 101, 1345–1359, 1996.

Guenther, A. B., Jiang, X., Heald, C. L., Sakulyanontvittaya, T., Duhl, T., Emmons, L. K., and Wang, X.: The Model of Emissions of Gases and Aerosols from Nature version 2.1 (MEGAN2.1): an extended and updated framework for modeling biogenic emissions, *Geoscientific Model Development*, 5, 1471–1492, 2012.

Han, Z.-W., Ueda, H., and Matsuda, K.: Model study of the impact of biogenic emission on regional ozone and the effectiveness of emission reduction scenarios over eastern China, *Tellus Ser. B Chem. Phys. Meteorol.*, 57, 12–27, 2005.

Hantson, S., Knorr, W., Schurgers, G., Pugh, T. A. M., and Arneth, A.: Global isoprene and monoterpene emissions under changing climate, vegetation, CO<sub>2</sub> and land use, *Atmospheric Environment*, 155, 35–45, 2017.

Hong, S.-Y., Noh, Y., and Dudhia, J.: A New Vertical Diffusion Package with an Explicit Treatment of Entrainment Processes, *Monthly Weather Review*, 134, 2318–2341, 2006.

Iacono, M. J., Delamere, J. S., Mlawer, E. J., Shephard, M. W., Clough, S. A., and Collins, W. D.: Radiative forcing by long-lived greenhouse gases: Calculations with the AER radiative transfer models, *Journal of Geophysical Research: Atmospheres*, 113, 2008.

Janssens Maenhout, G., Crippa, M., Guizzardi, D., Dentener, F., Muntean, M., Pouliot, G., Keating, T., Zhang, Q., Kurokawa, J., Wankmüller, R., van der Gon, H. D., Klimont, Z., Frost, G., Darras, S., and Koffi, B.: HTAP\_v2: a mosaic of regional and global emission gridmaps for 2008 and 2010 to study hemispheric transport of air pollution, *Atmospheric Chemistry & Physics Discussions*, 15, 12867–12909, 2015.

Jiang, F., Liu, Q., Huang, X., Wang, T., Zhuang, B., and Xie, M.: Regional modeling of secondary organic aerosol over China using WRF/Chem, *Journal of Aerosol Science*, 43, 57–73, 2012a.

Jiang, F., Zhou, P., Liu, Q., Wang, T., Zhuang, B., and Wang, X.: Modeling tropospheric ozone formation over East China in springtime, *Journal of Atmospheric Chemistry*, 69, 303–319, 2012b.

Jiang, X., Guenther, A., Potosnak, M., Geron, C., Seco, R., Karl, T., Kim, S., Gu, L., and Pallardy, S.: Isoprene Emission Response to Drought and the Impact on Global Atmospheric Chemistry, *Atmos Environ (1994)*, 183, 69–83, 2018.

Kain, J. S.: The Kain–Fritsch Convective Parameterization: An Update, *Journal of Applied Meteorology*, 43, 170–181, 2004.

Kim, S.-Y., Jiang, X., Lee, M., Turnipseed, A., Guenther, A., Kim, J.-C., Lee, S.-J., and Kim, S.: Impact of biogenic volatile organic compounds on ozone production at the Taehwa Research Forest near Seoul, South Korea, *Atmospheric Environment*, 70, 447–453, 2013.

- Kok, J. F.: A scaling theory for the size distribution of emitted dust aerosols suggests climate models underestimate the size of the global dust cycle, *Proceedings of the National Academy of Sciences*, 108, 1016, 2011.
- Kota, S. H., Schade, G., Estes, M., Boyer, D., and Ying, Q.: Evaluation of MEGAN predicted biogenic isoprene emissions at urban locations in Southeast Texas, *Atmospheric Environment*, 110, 54–64, 2015.
- Lehning, A., Zimmer, W., Zimmer, I., and Schnitzler, J. P.: Modeling of annual variations of oak (*Quercus robur* L.) isoprene synthase activity to predict isoprene emission rates, *Journal of Geophysical Research: Atmospheres*, 106, 3157–3166, 2001.
- Levis, S., Wiedinmyer, C., Bonan, G. B., and Guenther, A.: Simulating biogenic volatile organic compound emissions in the Community Climate System Model, *Journal of Geophysical Research: Atmospheres*, 108, 2003.
- Li, G., Bei, N., Cao, J., Wu, J., Long, X., Feng, T., Dai, W., Liu, S., Zhang, Q., and Tie, X.: Widespread and persistent ozone pollution in eastern China during the non-winter season of 2015: observations and source attributions, *Atmos. Chem. Phys.*, 17, 2759–2774, 2017a.
- Li, H., Li, L., Huang, C., An, J. y., Yan, R. s., Huang, H. y., Wang, Y. j., Lu, Q., Wang, Q., Lou, S. r., Wang, H. l., Zhou, M., Tao, S. k., Qiao, L. p., and Chen, M. h.: Ozone source apportionment at urban area during a typical photochemical pollution episode in the summer of 2013 in the Yangtze River Delta, *Huan jing ke xue= Huanjing kexue*, 36, 1–10, 2015a.
- Li, L., An, J. Y., Zhou, M., Yan, R. S., Huang, C., Lu, Q., Lin, L., Wang, Y. J., Tao, S. K., Qiao, L. P., Zhu, S. H., and Chen, C. H.: Source apportionment of fine particles and its chemical components over the Yangtze River Delta, China during a heavy haze pollution episode, *Atmospheric Environment*, 123, 415–429, 2015b.
- Li, L., Yang, W., Xie, S., and Wu, Y.: Estimations and uncertainty of biogenic volatile organic compound emission inventory in China for 2008–2018, *Science of The Total Environment*, 733, 139301, 2020.
- Li, L. Y. and Xie, S. D.: Historical variations of biogenic volatile organic compound emission inventories in China, 1981–2003, *Atmospheric Environment*, 95, 185–196, 2014.
- Li, M., Liu, H., Geng, G. N., Hong, C. P., Liu, F., Song, Y., Tong, D., Zheng, B., Cui, H. Y., Man, H. Y., Zhang, Q., and He, K. B.: Anthropogenic emission inventories in China: a review, *Natl. Sci. Rev.*, 4, 834–866, 2017b.
- Li, M., Zhang, Q., Kurokawa, J. I., Woo, J. H., He, K., Lu, Z., Ohara, T., Song, Y., Streets, D. G., Carmichael, G. R., Cheng, Y., Hong, C., Huo, H., Jiang, X., Kang, S., Liu, F., Su, H., and Zheng, B.: MIX: a mosaic Asian anthropogenic emission inventory under the international collaboration framework of the MICS Asia and HTAP, *Atmos. Chem. Phys.*, 17, 935–963, 2017c.
- Liu, Y., Li, L., An, J., Huang, L., Yan, R., Huang, C., Wang, H., Wang, Q., Wang, M., and Zhang, W.: Estimation of biogenic VOC emissions and its impact on ozone formation over the Yangtze River Delta region, China, *Atmospheric Environment*, 186, 113–128, 2018.

Loveland, T. R., Reed, B. C., Brown, J. F., Ohlen, D. O., Zhu, Z., Yang, L., and Merchant, J. W.: Development of a global land cover characteristics database and IGBP DISCover from 1 km AVHRR data, *Int. J. Remote Sens.*, 21, 1303–1330, 2000.

Lu, X., Zhang, L., Chen, Y., Zhou, M., Zheng, B., Li, K., Liu, Y., Lin, J., Fu, T. M., and Zhang, Q.: Exploring 2016–2017 surface ozone pollution over China: source contributions and meteorological influences, *Atmos. Chem. Phys.*, 19, 8339–8361, 2019.

Morrison, H., Thompson, G., and Tatarskii, V.: Impact of Cloud Microphysics on the Development of Trailing Stratiform Precipitation in a Simulated Squall Line: Comparison of One and Two Moment Schemes, *Monthly Weather Review*, 137, 991–1007, 2009.

Niinemets, Ü., Tenhunen, J. D., Harley, P. C., and Steinbrecher, R.: A model of isoprene emission based on energetic requirements for isoprene synthesis and leaf photosynthetic properties for Liquidambar and Quercus, *Plant, Cell & Environment*, 22, 1319–1335, 1999.

Oleson, K. W., Lawrence, D. M., Bonan, G. B., Flanner, M. G., Kluzek, E., and Lawrence, P. J.: Technical Description of version 4.0 of the Community Land Model (CLM), 2010–2010.

Paulson, C. A.: The mathematical representation of wind speed and temperature profiles in the unstable atmospheric surface layer, *J. Appl. Meteorol.*, 1970, 857–861, 1970.

Pierce, T., Geron, C., Bender, L., Dennis, R., Tonnesen, G., and Guenther, A.: Influence of increased isoprene emissions on regional ozone modeling, *Journal of Geophysical Research: Atmospheres*, 103, 25611–25629, 1998.

Poisson, N., Kanakidou, M., and Crutzen, P. J.: Impact of Non-Methane Hydrocarbons on Tropospheric Chemistry and the Oxidizing Power of the Global Troposphere: 3-Dimensional Modelling Results, *Journal of Atmospheric Chemistry*, 36, 157–230, 2000.

Safronov, A. N., Shtabkin, Y. A., Berezina, E. V., Skorokhod, A. I., Rakitin, V. S., Belikov, I. B., and Elansky, N. F.: Isoprene, Methyl Vinyl Ketone and Methacrolein from TROICA-12 Measurements and WRF-CHEM and GEOS-CHEM Simulations in the Far East Region, *Atmosphere*, 10, 26, 2019.

Situ, S., Guenther, A., Wang, X., Jiang, X., Turnipseed, A., Wu, Z., Bai, J., and Wang, X.: Impacts of seasonal and regional variability in biogenic VOC emissions on surface ozone in the Pearl River delta region, China, *Atmos. Chem. Phys.*, 13, 11803–11817, 2013.

Stauffer, D. R. and Seaman, N. L.: Use of Four Dimensional Data Assimilation in a Limited Area Mesoscale Model. Part I: Experiments with Synoptic Scale Data, *Monthly Weather Review*, 118, 1250–1277, 1990.

Stewart, H. E., Hewitt, C. N., Bunce, R. G. H., Steinbrecher, R., Smiatek, G., and Schoenemeyer, T.: A highly spatially and temporally resolved inventory for biogenic isoprene and monoterpene emissions: Model description and application to Great Britain, *Journal of Geophysical Research: Atmospheres*, 108, 2003.

Thenkabail, P. S., Knox, J. W., Ozdogan, M., Gumma, M. K., Congalton, R. G., Wu, Z.

T., Milesi, C., Finkral, A., Marshall, M., Mariotto, I., You, S. C., Giri, C., and Nagler, P.: ASSESSING FUTURE RISKS TO AGRICULTURAL PRODUCTIVITY, WATER RESOURCES AND FOOD SECURITY: HOW CAN REMOTE SENSING HELP, *Photogramm. Eng. Remote Sens.*, 78, 773–782, 2012.

Tie, X., Geng, F., Guenther, A., Cao, J., Greenberg, J., Zhang, R., Apel, E., Li, G., Weinheimer, A., Chen, J., and Cai, C.: Megacity impacts on regional ozone formation: observations and WRF Chem modeling for the MIRAGE Shanghai field campaign, *Atmos. Chem. Phys.*, 13, 5655–5669, 2013.

Visser, A. J., Boersma, K. F., Ganzeveld, L. N., and Krol, M. C.: European NO<sub>x</sub> emissions in WRF Chem derived from OMI: impacts on summertime surface ozone, *Atmos. Chem. Phys.*, 19, 11821–11841, 2019.

Wang, L. H., Follette Cook, M. B., Newchurch, M. J., Pickering, K. E., Pour Biazar, A., Kuang, S., Koshak, W., and Peterson, H.: Evaluation of lightning induced tropospheric ozone enhancements observed by ozone lidar and simulated by WRF/Chem, *Atmospheric Environment*, 115, 185–191, 2015.

Wang, Q. g., Han, Z., Wang, T., and Zhang, R.: Impacts of biogenic emissions of VOC and NO<sub>x</sub> on tropospheric ozone during summertime in eastern China, *Science of The Total Environment*, 395, 41–49, 2008.

Wang, R., Tie, X., Li, G., Zhao, S., Long, X., Johansson, L., and An, Z.: Effect of ship emissions on O<sub>3</sub> in the Yangtze River Delta region of China: Analysis of WRF-Chem modeling, *Science of The Total Environment*, 683, 360–370, 2019.

Wei, W., Lv, Z. F., Li, Y., Wang, L. T., Cheng, S. Y., and Liu, H.: A WRF Chem model study of the impact of VOCs emission of a huge petrochemical industrial zone on the summertime ozone in Beijing, China, *Atmospheric Environment*, 175, 44–53, 2018.

Wei, X. L., Li, Y. S., Lam, K. S., Wang, A. Y., and Wang, T. J.: Impact of biogenic VOC emissions on a tropical cyclone related ozone episode in the Pearl River Delta region, China, *Atmospheric Environment*, 41, 7851–7864, 2007.

Wiedinmyer, C., Akagi, S. K., Yokelson, R. J., Emmons, L. K., Al Saadi, J. A., Orlando, J. J., and Soja, A. J.: The Fire INventory from NCAR (FINN): a high resolution global model to estimate the emissions from open burning, *Geosci. Model Dev.*, 4, 625–641, 2011.

Wild, O., Zhu, X., and Prather, M. J.: Fast J: Accurate Simulation of In- and Below-Cloud Photolysis in Tropospheric Chemical Models, *Journal of Atmospheric Chemistry*, 37, 245–282, 2000.

Wu, K., Yang, X., Chen, D., Gu, S., Lu, Y., Jiang, Q., Wang, K., Ou, Y., Qian, Y., Shao, P., and Lu, S.: Estimation of biogenic VOC emissions and their corresponding impact on ozone and secondary organic aerosol formation in China, *Atmospheric Research*, 231, 104656, 2020.

Yang, Q., W. I. Gustafson, J., Fast, J. D., Wang, H., Easter, R. C., Morrison, H., Lee, Y. N., Chapman, E. G., Spak, S. N., and Mena Carrasco, M. A.: Assessing regional scale predictions of aerosols, marine stratocumulus, and their interactions during VOCALS REx using WRF Chem, *Atmos. Chem. Phys.*, 11, 11951–11975, 2011.

Yarwood, Wilson, G., Shepaed, S., and Guenther, A.: User's Guide to the Global

Biosphere Emissions and Interactions System (GloBEIS) Version3, 2002. 2002.

Yin, L., Xu, Z., Liu, M., Xu, T., Wang, T., Liao, W., Li, M., Cai, X., Kang, L., Zhang, H., and Song, Y.: Estimation of biogenic volatile organic compound (BVOC) emissions in China using WRF-CLM-MEGAN coupled model, *Biogeosciences Discuss.*, 2020, 1–30, 2020.

Zaveri, R. A. and Peters, L. K.: A new lumped structure photochemical mechanism for large scale applications, *Journal of Geophysical Research: Atmospheres*, 104, 30387–30415, 1999.

Zhang, L., Wang, T., Lv, M., and Zhang, Q.: On the severe haze in Beijing during January 2013: Unraveling the effects of meteorological anomalies with WRF-Chem, *Atmospheric Environment*, 104, 11–21, 2015.

Zhang, R., Suh, I., Lei, W., Clinkenbeard, A. D., and North, S. W.: Kinetic studies of OH initiated reactions of isoprene, *Journal of Geophysical Research: Atmospheres*, 105, 24627–24635, 2000.

Zhao, C., Chen, S., Leung, L. R., Qian, Y., Kok, J. F., Zaveri, R. A., and Huang, J.: Uncertainty in modeling dust mass balance and radiative forcing from size parameterization, *Atmos. Chem. Phys.*, 13, 10733–10753, 2013a.

Zhao, C., Hu, Z., Qian, Y., Ruby Leung, L., Huang, J., Huang, M., Jin, J., Flanner, M. G., Zhang, R., Wang, H., Yan, H., Lu, Z., and Streets, D. G.: Simulating black carbon and dust and their radiative forcing in seasonal snow: a case study over North China with field campaign measurements, *Atmos. Chem. Phys.*, 14, 11475–11491, 2014.

Zhao, C., Huang, M., Fast, J. D., Berg, L. K., Qian, Y., Guenther, A., Gu, D., Shrivastava, M., Liu, Y., Walters, S., Pfister, G., Jin, J., Shilling, J. E., and Warneke, C.: Sensitivity of biogenic volatile organic compounds to land surface parameterizations and vegetation distributions in California, *Geoscientific Model Development*, 9, 1959–1976, 2016.

Zhao, C., Liu, X., Leung, L. R., Johnson, B., McFarlane, S. A., Gustafson Jr, W. I., Fast, J. D., and Easter, R.: The spatial distribution of mineral dust and its shortwave radiative forcing over North Africa: modeling sensitivities to dust emissions and aerosol size treatments, *Atmos. Chem. Phys.*, 10, 8821–8838, 2010.

Zhao, C., Ruby Leung, L., Easter, R., Hand, J., and Avise, J.: Characterization of speciated aerosol direct radiative forcing over California, *Journal of Geophysical Research: Atmospheres*, 118, 2372–2388, 2013b.

Zhao, C., Wang, Y., and Zeng, T.: East China Plains: A “Basin” of Ozone Pollution, *Environmental Science & Technology*, 43, 1911–1915, 2009.

Zheng, J., Zheng, Z., Yu, Y., and Zhong, L.: Temporal, spatial characteristics and uncertainty of biogenic VOC emissions in the Pearl River Delta region, China, *Atmospheric Environment*, 44, 1960–1969, 2010.

Zhou, G., Xu, J., Xie, Y., Chang, L., Gao, W., Gu, Y., and Zhou, J.: Numerical air quality forecasting over eastern China: An operational application of WRF-Chem, *Atmospheric Environment*, 153, 94–108, 2017.

Zimmer, W., Steinbrecher, R., Körner, C., and Schnitzler, J. P.: The process-based SIM-BIM model: towards more realistic prediction of isoprene emissions from adult

- [Quercus petraea forest trees, Atmospheric Environment, 37, 1665–1671, 2003.](#)
- 
- [Abad, G. G., Vasilkov, A., Seftor, C., Liu, X., and Chance, K.: Smithsonian Astrophysical Observatory Ozone Mapping and Profiler Suite \(SAO OMPS\) formaldehyde retrieval, Atmos. Meas. Tech., 9, 2797–2812, 2016.](#)
- [Abdi-Oskouei, M., Pfister, G., Flocke, F., Sobhani, N., Saide, P., Fried, A., Richter, D., Weibring, P., Walega, J., and Carmichael, G.: Impacts of physical parameterization on prediction of ethane concentrations for oil and gas emissions in WRF-Chem, Atmos. Chem. Phys., 18, 16863–16883, 2018.](#)
- [Arghavani, S., Malakooti, H., and Bidokhti, A. A.: Numerical evaluation of urban green space scenarios effects on gaseous air pollutants in Tehran Metropolis based on WRF-Chem model, Atmospheric Environment, 214, 116832, 2019.](#)
- [Arneth, A., Niinemets, Ü., Pressley, S., Bäck, J., Hari, P., Karl, T., Noe, S., Prentice, I. C., Serça, D., Hickler, T., Wolf, A., and Smith, B.: Process-based estimates of terrestrial ecosystem isoprene emissions: incorporating the effects of a direct CO<sub>2</sub>-isoprene interaction, Atmos. Chem. Phys., 7, 31–53, 2007.](#)
- [Bao, H., Shrestha, K. L., Kondo, A., Kaga, A., and Inoue, Y.: Modeling the influence of biogenic volatile organic compound emissions on ozone concentration during summer season in the Kinki region of Japan, Atmospheric Environment, 44, 421–431, 2010.](#)
- [Bonan, G. B.: Land surface model \(LSM version 1.0\) for ecological, hydrological, and atmospheric studies: Technical description and user's guide. Technical note, United States, 1996.](#)
- [Brown, S. S., Dubé, W. P., Bahreini, R., Middlebrook, A. M., Brock, C. A., Warneke, C., de Gouw, J. A., Washenfelder, R. A., Atlas, E., Peischl, J., Ryerson, T. B., Holloway, J. S., Schwarz, J. P., Spackman, R., Trainer, M., Parrish, D. D., Fehsenfeld, F. C., and Ravishankara, A. R.: Biogenic VOC oxidation and organic aerosol formation in an urban nocturnal boundary layer: aircraft vertical profiles in Houston, TX, Atmos. Chem. Phys., 13, 11317–11337, 2013.](#)
- [Cai, C., Geng, F., Tie, X., Yu, Q., and An, J.: Characteristics and source apportionment of VOCs measured in Shanghai, China, Atmospheric Environment, 44, 5005–5014, 2010.](#)
- [Calfapietra, C., Fares, S., Manes, F., Morani, A., Sgrigna, G., and Loreto, F.: Role of Biogenic Volatile Organic Compounds \(BVOC\) emitted by urban trees on ozone concentration in cities: A review, Environmental Pollution, 183, 71–80, 2013.](#)
- [Carlton, A. G., Wiedinmyer, C., and Kroll, J. H.: A review of Secondary Organic Aerosol \(SOA\) formation from isoprene, Atmos. Chem. Phys., 9, 4987–5005, 2009.](#)
- [Carslaw, N., Bell, N., Lewis, A. C., McQuaid, J. B., and Pilling, M. J.: A detailed case study of isoprene chemistry during the EASE96 Mace Head campaign, Atmospheric Environment, 34, 2827–2836, 2000.](#)
- [Dentener, F., Kinne, S., Bond, T., Boucher, O., Cofala, J., Generoso, S., Ginoux, P., Gong, S., Hoelzemann, J. J., Ito, A., Marelli, L., Penner, J. E., Putaud, J. P., Textor, C., Schulz, M., van der Werf, G. R., and Wilson, J.: Emissions of primary aerosol and precursor gases in the years 2000 and 1750 prescribed data-sets for AeroCom,](#)



- Atmos. Chem. Phys., 6, 4321-4344, 2006.
- Derognat, C., Beekmann, M., Baeumle, M., Martin, D., and Schmidt, H.: Effect of biogenic volatile organic compound emissions on tropospheric chemistry during the Atmospheric Pollution Over the Paris Area (ESQUIF) campaign in the Ile-de-France region, *J. Geophys. Res.-Atmos.*, 108, 15, 2003.
- Fast, J. D., Gustafson Jr, W. I., Easter, R. C., Zaveri, R. A., Barnard, J. C., Chapman, E. G., Grell, G. A., and Peckham, S. E.: Evolution of ozone, particulates, and aerosol direct radiative forcing in the vicinity of Houston using a fully coupled meteorology-chemistry-aerosol model, *Journal of Geophysical Research: Atmospheres*, 111, 2006.
- Forkel, R., Balzarini, A., Baró, R., Bianconi, R., Curci, G., Jiménez-Guerrero, P., Hirtl, M., Honzak, L., Lorenz, C., Im, U., Pérez, J. L., Pirovano, G., San José, R., Tuccella, P., Werhahn, J., and Žabkar, R.: Analysis of the WRF-Chem contributions to AQMEII phase2 with respect to aerosol radiative feedbacks on meteorology and pollutant distributions, *Atmospheric Environment*, 115, 630-645, 2015.
- Friedl, M. A., McIver, D. K., Hodges, J. C. F., Zhang, X. Y., Muchoney, D., Strahler, A. H., Woodcock, C. E., Gopal, S., Schneider, A., Cooper, A., Baccini, A., Gao, F., and Schaaf, C.: Global land cover mapping from MODIS: algorithms and early results, *Remote Sensing of Environment*, 83, 287-302, 2002.
- Fu, P., Kawamura, K., Kanaya, Y., and Wang, Z.: Contributions of biogenic volatile organic compounds to the formation of secondary organic aerosols over Mt. Tai, Central East China, *Atmospheric Environment*, 44, 4817-4826, 2010.
- Geng, F., Tie, X., Guenther, A., Li, G., Cao, J., and Harley, P.: Effect of isoprene emissions from major forests on ozone formation in the city of Shanghai, China, *Atmos. Chem. Phys.*, 11, 10449-10459, 2011.
- Geron, C. D., Guenther, A. B., and Pierce, T. E.: An improved model for estimating emissions of volatile organic compounds from forests in the eastern United States, *Journal of Geophysical Research: Atmospheres*, 99, 12773-12791, 1994.
- Ghude, S. D., Pfister, G. G., Jena, C., van der A, R. J., Emmons, L. K., and Kumar, R.: Satellite constraints of nitrogen oxide (NO<sub>x</sub>) emissions from India based on OMI observations and WRF-Chem simulations, *Geophysical Research Letters*, 40, 423-428, 2013.
- Ginoux, P., Chin, M., Tegen, I., Prospero, J. M., Holben, B., Dubovik, O., and Lin, S.-J.: Sources and distributions of dust aerosols simulated with the GOCART model, *Journal of Geophysical Research: Atmospheres*, 106, 20255-20273, 2001.
- Gregorio, A.: Land Cover Classification System (LCCS), version 2: Classification Concepts and User Manual: LCCS, Number8. Food & Agriculture Organization, Rome, Italy., FAO Environment and Natural Resources Service Series, 8, 2005.
- Grell, G. A., Peckham, S. E., Schmitz, R., McKeen, S. A., Frost, G., Skamarock, W. C., and Eder, B.: Fully coupled "online" chemistry within the WRF model, *Atmospheric Environment*, 39, 6957-6975, 2005.
- Guenther, A.: Biological and Chemical Diversity of Biogenic Volatile Organic Emissions into the Atmosphere, *ISRN Atmospheric Sciences*, 2013, 2013.



Guenther, A.: Estimates of global terrestrial isoprene emissions using MEGAN (Model of Emissions of Gases and Aerosols from Nature) (vol 6, pg 3181, 2006), *Atmos. Chem. Phys.*, 7, 4327-4327, 2006.

Guenther, A., Hewitt, C. N., Erickson, D., Fall, R., Geron, C., Graedel, T., Harley, P., Klinger, L., Lerdau, M., McKay, W. A., Pierce, T., Scholes, B., Steinbrecher, R., Tallamraju, R., Taylor, J., and Zimmerman, P.: A global model of natural volatile organic compound emissions, *Journal of Geophysical Research: Atmospheres*, 100, 8873-8892, 1995.

Guenther, A., Zimmerman, P., Klinger, L., Greenberg, J., Ennis, C., Davis, K., Pollock, W., Westberg, H., Allwine, G., and Geron, C.: Estimates of regional natural volatile organic compound fluxes from enclosure and ambient measurements, *J. Geophys. Res.-Atmos.*, 101, 1345-1359, 1996.

Guenther, A. B., Jiang, X., Heald, C. L., Sakulyanontvittaya, T., Duhl, T., Emmons, L. K., and Wang, X.: The Model of Emissions of Gases and Aerosols from Nature version 2.1 (MEGAN2.1): an extended and updated framework for modeling biogenic emissions, *Geoscientific Model Development*, 5, 1471-1492, 2012.

Han, Z. W., Ueda, H., and Matsuda, K.: Model study of the impact of biogenic emission on regional ozone and the effectiveness of emission reduction scenarios over eastern China, *Tellus Ser. B-Chem. Phys. Meteorol.*, 57, 12-27, 2005.

Hantson, S., Knorr, W., Schurgers, G., Pugh, T. A. M., and Arneth, A.: Global isoprene and monoterpene emissions under changing climate, vegetation, CO<sub>2</sub> and land use, *Atmospheric Environment*, 155, 35-45, 2017.

Hong, S.-Y., Noh, Y., and Dudhia, J.: A New Vertical Diffusion Package with an Explicit Treatment of Entrainment Processes, *Monthly Weather Review*, 134, 2318-2341, 2006.

Iacono, M. J., Delamere, J. S., Mlawer, E. J., Shephard, M. W., Clough, S. A., and Collins, W. D.: Radiative forcing by long-lived greenhouse gases: Calculations with the AER radiative transfer models, *Journal of Geophysical Research: Atmospheres*, 113, 2008.

Janssens-Maenhout, G., Crippa, M., Guizzardi, D., Dentener, F., Muntean, M., Pouliot, G., Keating, T., Zhang, Q., Kurokawa, J., Wankmüller, R., van der Gon, H. D., Klimont, Z., Frost, G., Darras, S., and Koffi, B.: HTAP v2: a mosaic of regional and global emission gridmaps for 2008 and 2010 to study hemispheric transport of air pollution, *Atmospheric Chemistry & Physics Discussions*, 15, 12867-12909, 2015.

Jiang, F., Liu, Q., Huang, X., Wang, T., Zhuang, B., and Xie, M.: Regional modeling of secondary organic aerosol over China using WRF/Chem, *Journal of Aerosol Science*, 43, 57-73, 2012a.

Jiang, F., Zhou, P., Liu, Q., Wang, T., Zhuang, B., and Wang, X.: Modeling tropospheric ozone formation over East China in springtime, *Journal of Atmospheric Chemistry*, 69, 303-319, 2012b.

Jiang, X., Guenther, A., Potosnak, M., Geron, C., Seco, R., Karl, T., Kim, S., Gu, L., and Pallardy, S.: Isoprene Emission Response to Drought and the Impact on Global Atmospheric Chemistry, *Atmos Environ* (1994), 183, 69-83, 2018.

- Kain, J. S.: The Kain–Fritsch Convective Parameterization: An Update, *Journal of Applied Meteorology*, 43, 170-181, 2004.
- Kim, S.-Y., Jiang, X., Lee, M., Turnipseed, A., Guenther, A., Kim, J.-C., Lee, S.-J., and Kim, S.: Impact of biogenic volatile organic compounds on ozone production at the Taehwa Research Forest near Seoul, South Korea, *Atmospheric Environment*, 70, 447-453, 2013.
- Kok, J. F.: A scaling theory for the size distribution of emitted dust aerosols suggests climate models underestimate the size of the global dust cycle, *Proceedings of the National Academy of Sciences*, 108, 1016, 2011.
- Kota, S. H., Schade, G., Estes, M., Boyer, D., and Ying, Q.: Evaluation of MEGAN predicted biogenic isoprene emissions at urban locations in Southeast Texas, *Atmospheric Environment*, 110, 54-64, 2015.
- Lehning, A., Zimmer, W., Zimmer, I., and Schnitzler, J. P.: Modeling of annual variations of oak (*Quercus robur* L.) isoprene synthase activity to predict isoprene emission rates, *Journal of Geophysical Research: Atmospheres*, 106, 3157-3166, 2001.
- Levis, S., Wiedinmyer, C., Bonan, G. B., and Guenther, A.: Simulating biogenic volatile organic compound emissions in the Community Climate System Model, *Journal of Geophysical Research: Atmospheres*, 108, 2003.
- Li, G., Bei, N., Cao, J., Wu, J., Long, X., Feng, T., Dai, W., Liu, S., Zhang, Q., and Tie, X.: Widespread and persistent ozone pollution in eastern China during the non-winter season of 2015: observations and source attributions, *Atmos. Chem. Phys.*, 17, 2759-2774, 2017a.
- Li, H., Li, L., Huang, C., An, J.-y., Yan, R.-s., Huang, H.-y., Wang, Y.-j., Lu, Q., Wang, Q., Lou, S.-r., Wang, H.-l., Zhou, M., Tao, S.-k., Qiao, L.-p., and Chen, M.-h.: Ozone source apportionment at urban area during a typical photochemical pollution episode in the summer of 2013 in the Yangtze River Delta, *Huan jing ke xue= Huanjing kexue*, 36, 1-10, 2015a.
- Li, L., An, J. Y., Zhou, M., Yan, R. S., Huang, C., Lu, Q., Lin, L., Wang, Y. J., Tao, S. K., Qiao, L. P., Zhu, S. H., and Chen, C. H.: Source apportionment of fine particles and its chemical components over the Yangtze River Delta, China during a heavy haze pollution episode, *Atmospheric Environment*, 123, 415-429, 2015b.
- Li, L., Yang, W., Xie, S., and Wu, Y.: Estimations and uncertainty of biogenic volatile organic compound emission inventory in China for 2008–2018, *Science of The Total Environment*, 733, 139301, 2020.
- Li, L. Y. and Xie, S. D.: Historical variations of biogenic volatile organic compound emission inventories in China, 1981–2003, *Atmospheric Environment*, 95, 185-196, 2014.
- Li, M., Liu, H., Geng, G. N., Hong, C. P., Liu, F., Song, Y., Tong, D., Zheng, B., Cui, H. Y., Man, H. Y., Zhang, Q., and He, K. B.: Anthropogenic emission inventories in China: a review, *Natl. Sci. Rev.*, 4, 834-866, 2017b.
- Li, M., Zhang, Q., Kurokawa, J. I., Woo, J. H., He, K., Lu, Z., Ohara, T., Song, Y., Streets, D. G., Carmichael, G. R., Cheng, Y., Hong, C., Huo, H., Jiang, X., Kang, S., Liu, F., Su, H., and Zheng, B.: MIX: a mosaic Asian anthropogenic emission

inventory under the international collaboration framework of the MICS-Asia and HTAP, *Atmos. Chem. Phys.*, 17, 935-963, 2017c.

Li, X., Cai, C., Zhu, B., An, J., Li, Y., and Li, Y.: Source apportionment of VOCs in a suburb of Nanjing, China, in autumn and winter, *Journal of Atmospheric Chemistry*, 71, 175-193, 2014.

Liu, Y., Li, L., An, J., Huang, L., Yan, R., Huang, C., Wang, H., Wang, Q., Wang, M., and Zhang, W.: Estimation of biogenic VOC emissions and its impact on ozone formation over the Yangtze River Delta region, China, *Atmospheric Environment*, 186, 113-128, 2018.

Loveland, T. R., Reed, B. C., Brown, J. F., Ohlen, D. O., Zhu, Z., Yang, L., and Merchant, J. W.: Development of a global land cover characteristics database and IGBP DISCover from 1 km AVHRR data, *Int. J. Remote Sens.*, 21, 1303-1330, 2000.

Lu, X., Zhang, L., Chen, Y., Zhou, M., Zheng, B., Li, K., Liu, Y., Lin, J., Fu, T. M., and Zhang, Q.: Exploring 2016–2017 surface ozone pollution over China: source contributions and meteorological influences, *Atmos. Chem. Phys.*, 19, 8339-8361, 2019.

Lyu, X. P., Chen, N., Guo, H., Zhang, W. H., Wang, N., Wang, Y., and Liu, M.: Ambient volatile organic compounds and their effect on ozone production in Wuhan, central China, *Science of the Total Environment*, 541, 200-209, 2016.

Morrison, H., Thompson, G., and Tatarskii, V.: Impact of Cloud Microphysics on the Development of Trailing Stratiform Precipitation in a Simulated Squall Line: Comparison of One- and Two-Moment Schemes, *Monthly Weather Review*, 137, 991-1007, 2009.

Niinemets, Ü., Tenhunen, J. D., Harley, P. C., and Steinbrecher, R.: A model of isoprene emission based on energetic requirements for isoprene synthesis and leaf photosynthetic properties for Liquidambar and Quercus, *Plant, Cell & Environment*, 22, 1319-1335, 1999.

Oleson, K. W., Lawrence, D. M., Bonan, G. B., Flanner, M. G., Kluzek, E., and Lawrence, P. J.: Technical Description of version 4.0 of the Community Land Model (CLM), 2010. 2010.

Paulson, C. A.: The mathematical representation of wind speed and temperature profiles in the unstable atmospheric surface layer, *J. Appl. Meteorol.*, 1970. 857-861, 1970.

Pierce, T., Geron, C., Bender, L., Dennis, R., Tonnesen, G., and Guenther, A.: Influence of increased isoprene emissions on regional ozone modeling, *Journal of Geophysical Research: Atmospheres*, 103, 25611-25629, 1998.

Poisson, N., Kanakidou, M., and Crutzen, P. J.: Impact of Non-Methane Hydrocarbons on Tropospheric Chemistry and the Oxidizing Power of the Global Troposphere: 3-Dimensional Modelling Results, *Journal of Atmospheric Chemistry*, 36, 157-230, 2000.

Safronov, A. N., Shtabkin, Y. A., Berezina, E. V., Skorokhod, A. I., Rakitin, V. S., Belikov, I. B., and Elansky, N. F.: Isoprene, Methyl Vinyl Ketone and Methacrolein from TROICA-12 Measurements and WRF-CHEM and GEOS-CHEM Simulations in the Far East Region, *Atmosphere*, 10, 26, 2019.

- Shao, P., An, J., Xin, J., Wu, F., Wang, J., Ji, D., and Wang, Y.: Source apportionment of VOCs and the contribution to photochemical ozone formation during summer in the typical industrial area in the Yangtze River Delta, China, *Atmospheric Research*, 176-177, 64-74, 2016.
- Situ, S., Guenther, A., Wang, X., Jiang, X., Turnipseed, A., Wu, Z., Bai, J., and Wang, X.: Impacts of seasonal and regional variability in biogenic VOC emissions on surface ozone in the Pearl River delta region, China, *Atmos. Chem. Phys.*, 13, 11803-11817, 2013.
- Stauffer, D. R. and Seaman, N. L.: Use of Four-Dimensional Data Assimilation in a Limited-Area Mesoscale Model. Part I: Experiments with Synoptic-Scale Data, *Monthly Weather Review*, 118, 1250-1277, 1990.
- Stewart, H. E., Hewitt, C. N., Bunce, R. G. H., Steinbrecher, R., Smiatek, G., and Schoenemeyer, T.: A highly spatially and temporally resolved inventory for biogenic isoprene and monoterpene emissions: Model description and application to Great Britain, *Journal of Geophysical Research: Atmospheres*, 108, 2003.
- Su, W. J., Liu, C., Chan, K. L., Hu, Q. H., Liu, H. R., Ji, X. G., Zhu, Y. Z., Liu, T., Zhang, C. X., Chen, Y. J., and Liu, J. G.: An improved TROPOMI tropospheric HCHO retrieval over China, *Atmos. Meas. Tech.*, 13, 6271-6292, 2020.
- Su, W. J., Liu, C., Hu, Q. H., Zhao, S. H., Sun, Y. W., Wang, W., Zhu, Y. Z., Liu, J. G., and Kim, J.: Primary and secondary sources of ambient formaldehyde in the Yangtze River Delta based on Ozone Mapping and Profiler Suite (OMPS) observations, *Atmos. Chem. Phys.*, 19, 6717-6736, 2019.
- Thenkabail, P. S., Knox, J. W., Ozdogan, M., Gumma, M. K., Congalton, R. G., Wu, Z. T., Milesi, C., Finkral, A., Marshall, M., Mariotto, I., You, S. C., Giri, C., and Nagler, P.: ASSESSING FUTURE RISKS TO AGRICULTURAL PRODUCTIVITY, WATER RESOURCES AND FOOD SECURITY: HOW CAN REMOTE SENSING HELP?, *Photogramm. Eng. Remote Sens.*, 78, 773-782, 2012.
- Tie, X., Geng, F., Guenther, A., Cao, J., Greenberg, J., Zhang, R., Apel, E., Li, G., Weinheimer, A., Chen, J., and Cai, C.: Megacity impacts on regional ozone formation: observations and WRF-Chem modeling for the MIRAGE-Shanghai field campaign, *Atmos. Chem. Phys.*, 13, 5655-5669, 2013.
- Visser, A. J., Boersma, K. F., Ganzeveld, L. N., and Krol, M. C.: European NO<sub>x</sub> emissions in WRF-Chem derived from OMI: impacts on summertime surface ozone, *Atmos. Chem. Phys.*, 19, 11821-11841, 2019.
- Wang, L. H., Follette-Cook, M. B., Newchurch, M. J., Pickering, K. E., Pour-Biazar, A., Kuang, S., Koshak, W., and Peterson, H.: Evaluation of lightning-induced tropospheric ozone enhancements observed by ozone lidar and simulated by WRF/Chem, *Atmospheric Environment*, 115, 185-191, 2015.
- Wang, Q. g., Han, Z., Wang, T., and Zhang, R.: Impacts of biogenic emissions of VOC and NO<sub>x</sub> on tropospheric ozone during summertime in eastern China, *Science of The Total Environment*, 395, 41-49, 2008.
- Wang, R., Tie, X., Li, G., Zhao, S., Long, X., Johansson, L., and An, Z.: Effect of ship emissions on O<sub>3</sub> in the Yangtze River Delta region of China: Analysis of WRF-

- Chem modeling, *Science of The Total Environment*, 683, 360-370, 2019.
- Wei, W., Lv, Z. F., Li, Y., Wang, L. T., Cheng, S. Y., and Liu, H.: A WRF-Chem model study of the impact of VOCs emission of a huge petrochemical industrial zone on the summertime ozone in Beijing, China, *Atmospheric Environment*, 175, 44-53, 2018.
- Wei, X. L., Li, Y. S., Lam, K. S., Wang, A. Y., and Wang, T. J.: Impact of biogenic VOC emissions on a tropical cyclone-related ozone episode in the Pearl River Delta region, China, *Atmospheric Environment*, 41, 7851-7864, 2007.
- Wiedinmyer, C., Akagi, S. K., Yokelson, R. J., Emmons, L. K., Al-Saadi, J. A., Orlando, J. J., and Soja, A. J.: The Fire INventory from NCAR (FINN): a high resolution global model to estimate the emissions from open burning, *Geosci. Model Dev.*, 4, 625-641, 2011.
- Wild, O., Zhu, X., and Prather, M. J.: Fast-J: Accurate Simulation of In- and Below-Cloud Photolysis in Tropospheric Chemical Models, *Journal of Atmospheric Chemistry*, 37, 245-282, 2000.
- Wu, K., Yang, X., Chen, D., Gu, S., Lu, Y., Jiang, Q., Wang, K., Ou, Y., Qian, Y., Shao, P., and Lu, S.: Estimation of biogenic VOC emissions and their corresponding impact on ozone and secondary organic aerosol formation in China, *Atmospheric Research*, 231, 104656, 2020.
- Yang, Q., W. I. Gustafson, J., Fast, J. D., Wang, H., Easter, R. C., Morrison, H., Lee, Y. N., Chapman, E. G., Spak, S. N., and Mena-Carrasco, M. A.: Assessing regional scale predictions of aerosols, marine stratocumulus, and their interactions during VOCALS-REx using WRF-Chem, *Atmos. Chem. Phys.*, 11, 11951-11975, 2011.
- Yarwood, Wilson, G., Shepaed, S., and Guenther, A.: User's Guide to the Global Biosphere Emissions and Interactions System (GloBEIS) Version3, 2002. 2002.
- Yin, L., Xu, Z., Liu, M., Xu, T., Wang, T., Liao, W., Li, M., Cai, X., Kang, L., Zhang, H., and Song, Y.: Estimation of biogenic volatile organic compound (BVOC) emissions in China using WRF-CLM-MEGAN coupled model, *Biogeosciences Discuss.*, 2020, 1-30, 2020.
- Zaveri, R. A. and Peters, L. K.: A new lumped structure photochemical mechanism for large-scale applications, *Journal of Geophysical Research: Atmospheres*, 104, 30387-30415, 1999.
- Zhang, L., Wang, T., Lv, M., and Zhang, Q.: On the severe haze in Beijing during January 2013: Unraveling the effects of meteorological anomalies with WRF-Chem, *Atmospheric Environment*, 104, 11-21, 2015.
- Zhang, R., Suh, I., Lei, W., Clinkenbeard, A. D., and North, S. W.: Kinetic studies of OH-initiated reactions of isoprene, *Journal of Geophysical Research: Atmospheres*, 105, 24627-24635, 2000.
- Zhao, C., Chen, S., Leung, L. R., Qian, Y., Kok, J. F., Zaveri, R. A., and Huang, J.: Uncertainty in modeling dust mass balance and radiative forcing from size parameterization, *Atmos. Chem. Phys.*, 13, 10733-10753, 2013a.
- Zhao, C., Hu, Z., Qian, Y., Ruby Leung, L., Huang, J., Huang, M., Jin, J., Flanner, M. G., Zhang, R., Wang, H., Yan, H., Lu, Z., and Streets, D. G.: Simulating black carbon and dust and their radiative forcing in seasonal snow: a case study over

North China with field campaign measurements, *Atmos. Chem. Phys.*, 14, 11475-11491, 2014.

Zhao, C., Huang, M., Fast, J. D., Berg, L. K., Qian, Y., Guenther, A., Gu, D., Shrivastava, M., Liu, Y., Walters, S., Pfister, G., Jin, J., Shilling, J. E., and Warneke, C.: Sensitivity of biogenic volatile organic compounds to land surface parameterizations and vegetation distributions in California, *Geoscientific Model Development*, 9, 1959-1976, 2016.

Zhao, C., Liu, X., Leung, L. R., Johnson, B., McFarlane, S. A., Gustafson Jr, W. I., Fast, J. D., and Easter, R.: The spatial distribution of mineral dust and its shortwave radiative forcing over North Africa: modeling sensitivities to dust emissions and aerosol size treatments, *Atmos. Chem. Phys.*, 10, 8821-8838, 2010.

Zhao, C., Ruby Leung, L., Easter, R., Hand, J., and Avise, J.: Characterization of speciated aerosol direct radiative forcing over California, *Journal of Geophysical Research: Atmospheres*, 118, 2372-2388, 2013b.

Zhao, C., Wang, Y., and Zeng, T.: East China Plains: A “Basin” of Ozone Pollution, *Environmental Science & Technology*, 43, 1911-1915, 2009.

Zheng, J., Zheng, Z., Yu, Y., and Zhong, L.: Temporal, spatial characteristics and uncertainty of biogenic VOC emissions in the Pearl River Delta region, China, *Atmospheric Environment*, 44, 1960-1969, 2010.

Zhou, G., Xu, J., Xie, Y., Chang, L., Gao, W., Gu, Y., and Zhou, J.: Numerical air quality forecasting over eastern China: An operational application of WRF-Chem, *Atmospheric Environment*, 153, 94-108, 2017.

Zimmer, W., Steinbrecher, R., Körner, C., and Schnitzler, J. P.: The process-based SIM-BIM model: towards more realistic prediction of isoprene emissions from adult *Quercus petraea* forest trees, *Atmospheric Environment*, 37, 1665-1671, 2003.

带格式的: 缩进: 左侧: 0 厘米, 首行缩进: 0 字符

带格式的: 缩进: 左侧: 0 厘米, 首行缩进: 0 字符

带格式的: 缩进: 左侧: 0 厘米, 首行缩进: 0 字符

1525  
1526  
1527  
1528  
1529  
1530  
1531  
1532  
1533  
1534  
1535  
1536  
1537  
1538  
1539  
1540  
1541  
1542  
1543  
1544  
1545  
1546  
1547  
1548

带格式的: 缩进: 左侧: 0 厘米, 首行缩进: 0 字符

带格式的: 居中, 缩进: 左侧: 0 厘米, 首行缩进: 0 字符



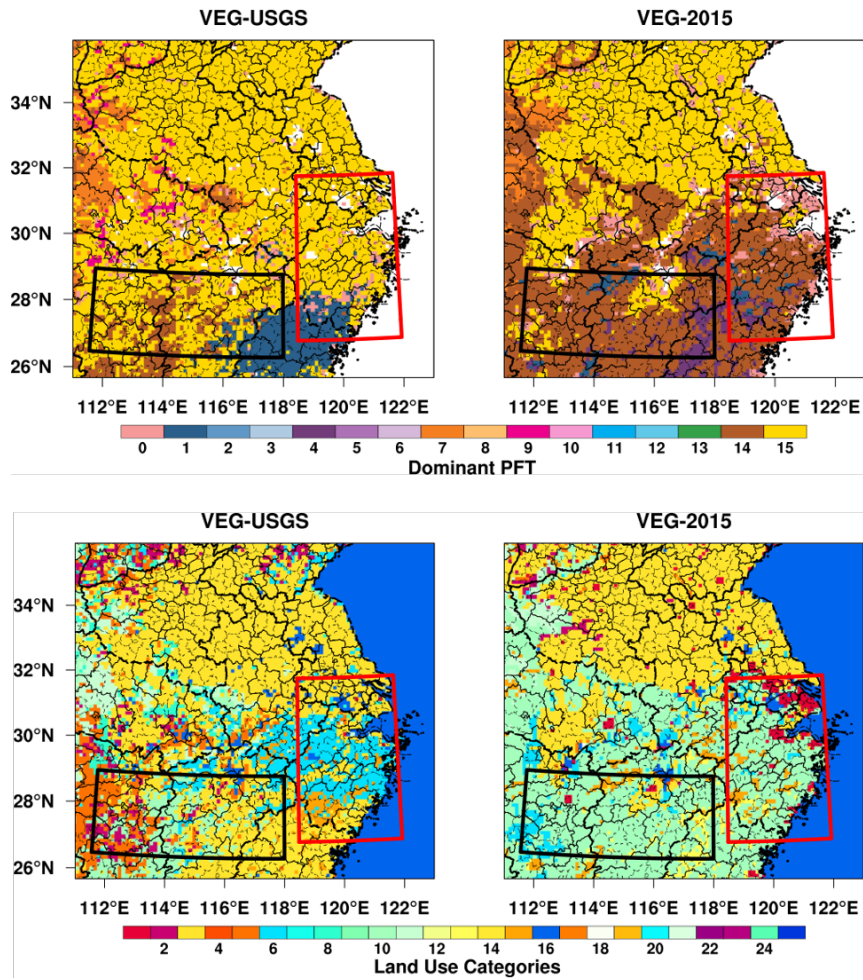


**Figure 1.** Spatial distribution of two different vegetation data sets (VEG-USGS and VEG-2015) and dominant PFT derived from them in each grid over the simulation domain.



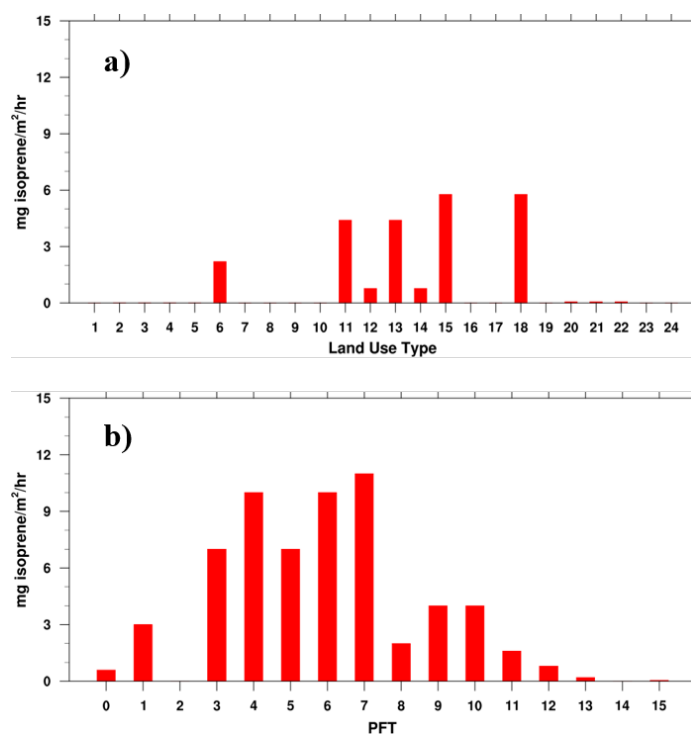
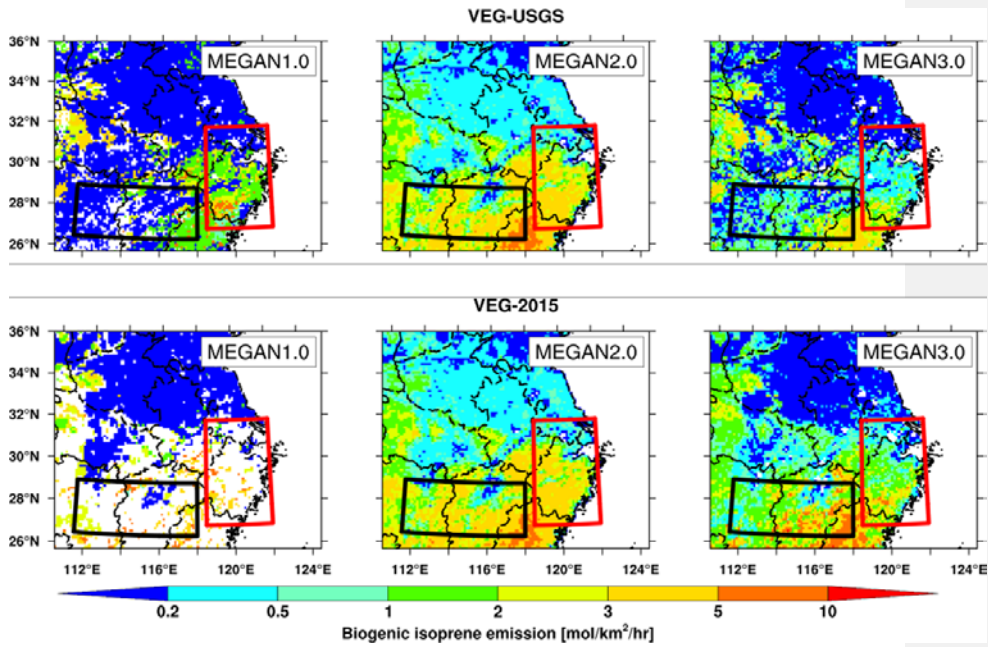


**Figure 2.** Biogenic emission factor for each land use category in (a) MEGAN v1.0, and the land use number 1-24 detailed describe can be found in Table 3 and (b) for each PFT in MEGAN v3.0, the PFT number 0-15 are listed in Table 42.

1581



1582

1583 **Figure 3.** Spatial distributions of biogenic isoprene emissions averaged in April over  
1584 the simulation domain estimated with different biogenic emission scheme and  
1585 vegetation data set as listed in Table 42. Two areas are marked by red and black box  
1586 to discuss the characters in detail.

1587

1588

1589

1590

1591

1592

1593

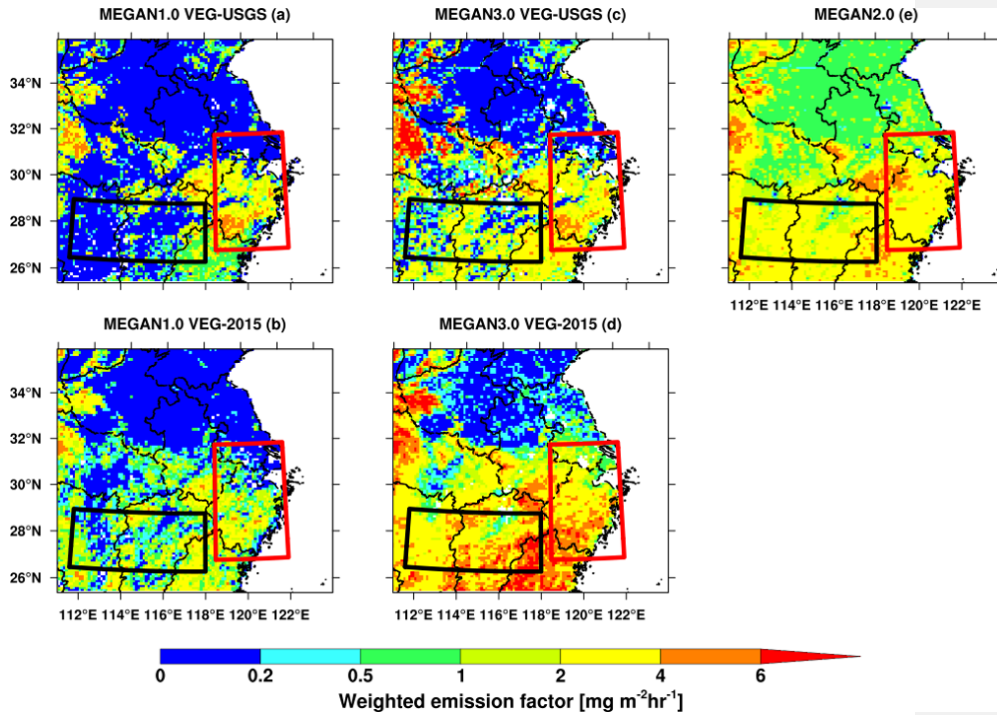
1594

1595

1596

1597

1598



1599

1600 **Figure 4.** Spatial distribution of the weighted mean emission factor derived from  
 1601 VEG-USGS and VEG-2015 in MEGAN v1.0 (a)(b) and MEGAN v3.0 (c)(d).  
 1602 Meanwhile, (e) shows the distribution of isoprene emission factor in MEGAN v2.0  
 1603 database. [Please note the emission factors of isoprene are prescribed for](#)  
 1604 [MEGANv2.0 in WRF-Chem and therefore are independent on vegetation](#)  
 1605 [distributions.](#)

1606

1607

1608

1609

1610

1611

1612

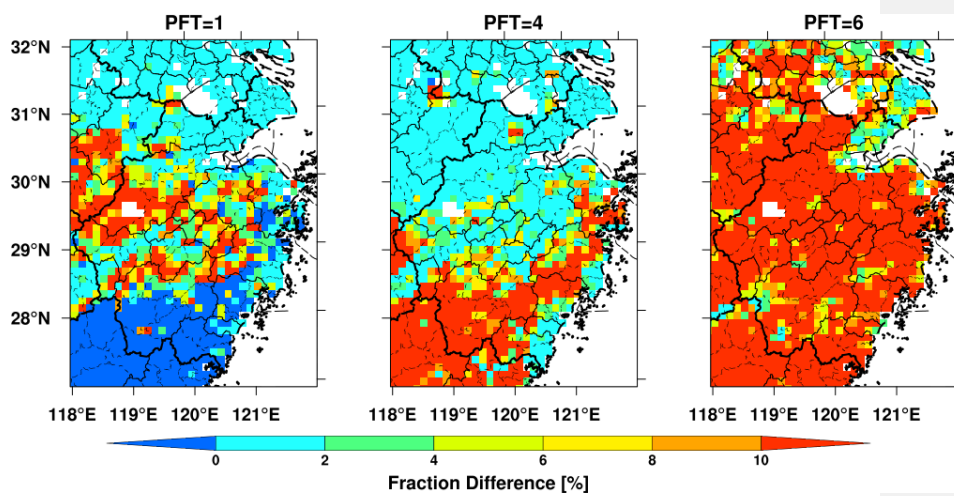


**Figure 5.** Spatial distribution of the PFT percentage difference between the VEG-2015 and VEG-USGS (VEG-2015 minus VEG-USGS) for needle-leaf evergreen tree, [\(PFT=1\)](#), broadleaf evergreen tree [\(PFT=4\)](#) and broadleaf deciduous tree, [\(PFT=6\)](#).

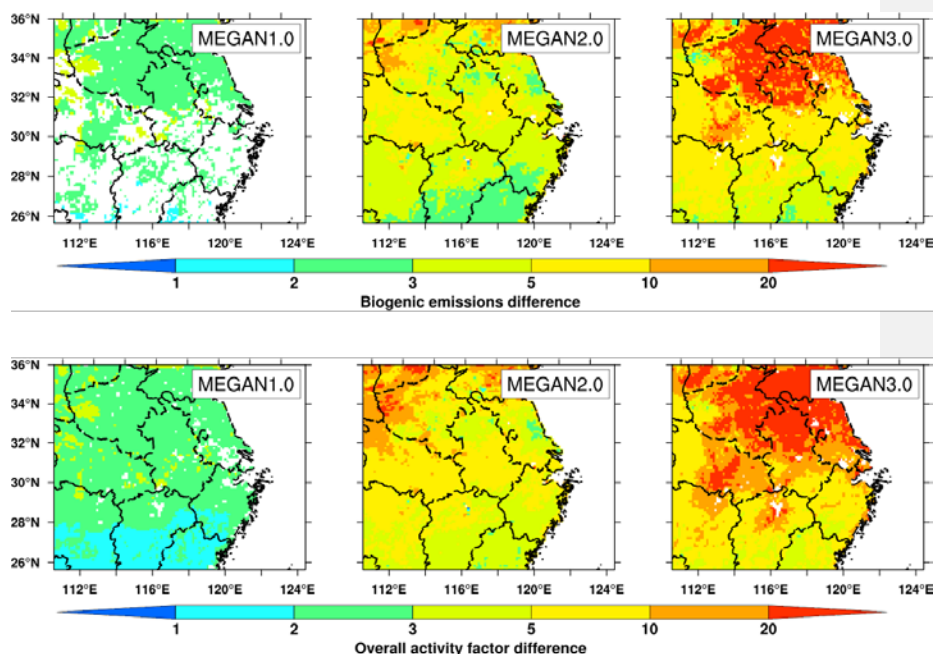
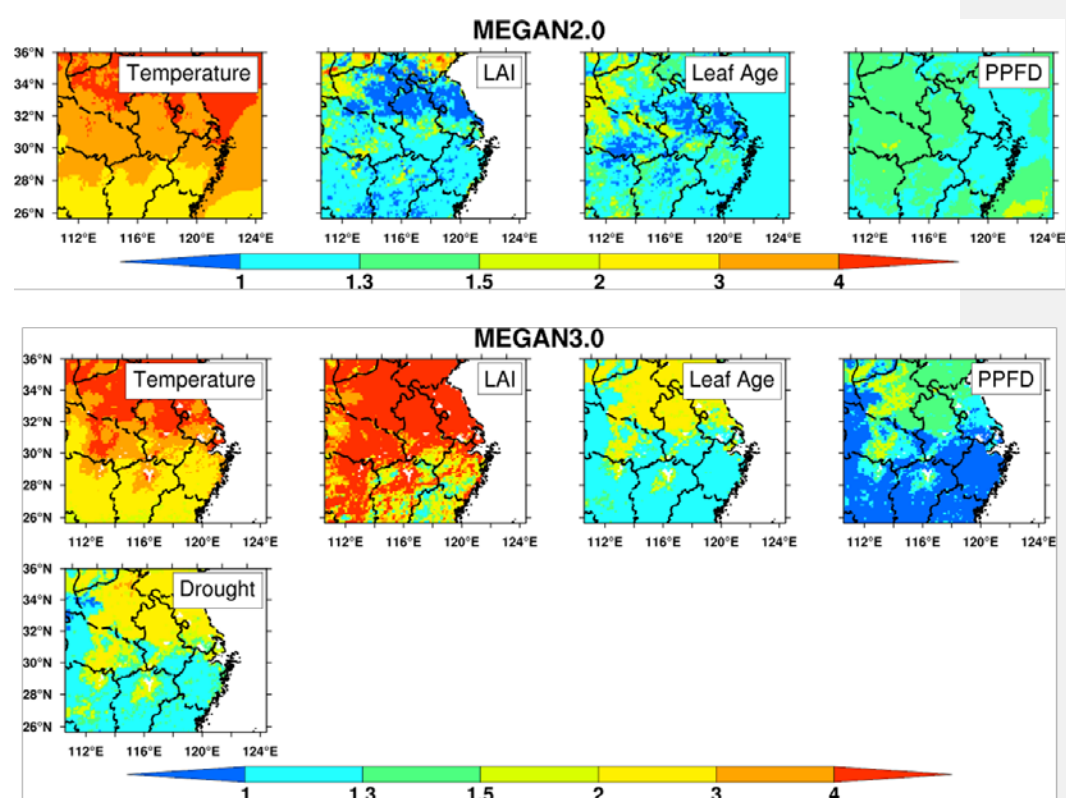


**Figure 6.** Spatial distribution of the quotient of biogenic isoprene emission and activity factor between simulations [in July and that in April](#), using VEG-2015 vegetation data set [in July and that in April](#), coupled with different emission schemes ([MEGANv1.0](#), [MEGANv2.0](#) and [MEGANv3.0](#)).

1651  
1652



1653  
1654  
1655  
1656  
1657  
1658  
1659  
1660  
1661  
1662  
1663

**Figure 7.** Spatial distribution of the quotient of activity factor related to different environmental variables (such as temperature, LAI, light, leaf age and drought) between simulations in July and that in April (July divided by April) using VEG-2015 vegetation data set coupled with MEGAN v2.0 and MEGAN v3.0.

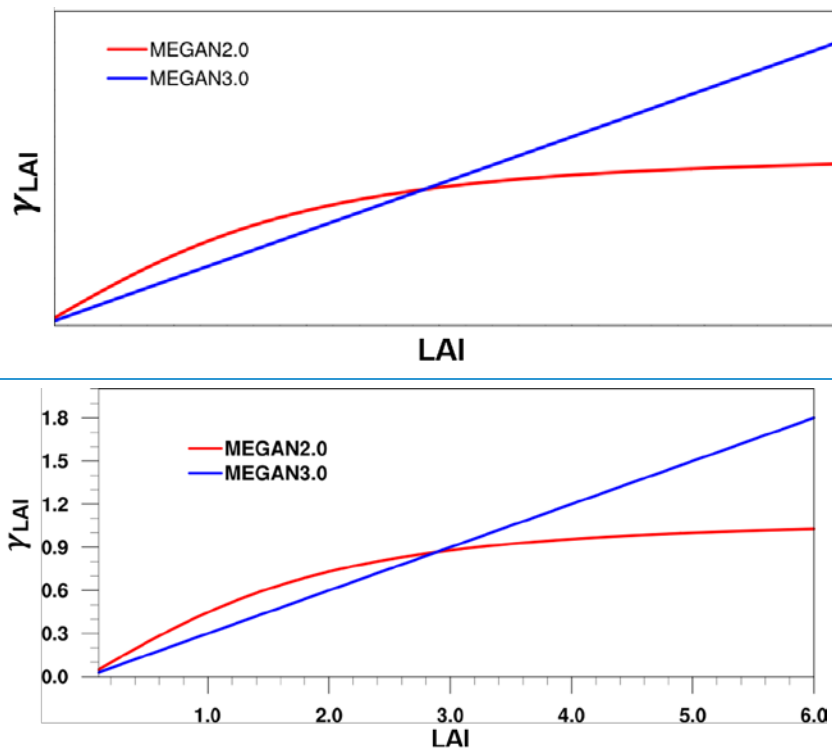


**Figure 8.** Activity factor for LAI ( $\gamma_{LAI}$ ) variation with LAI in different versions of MEGAN, red line represent the MEGAN v2.0 and blue line for MEGAN v3.0

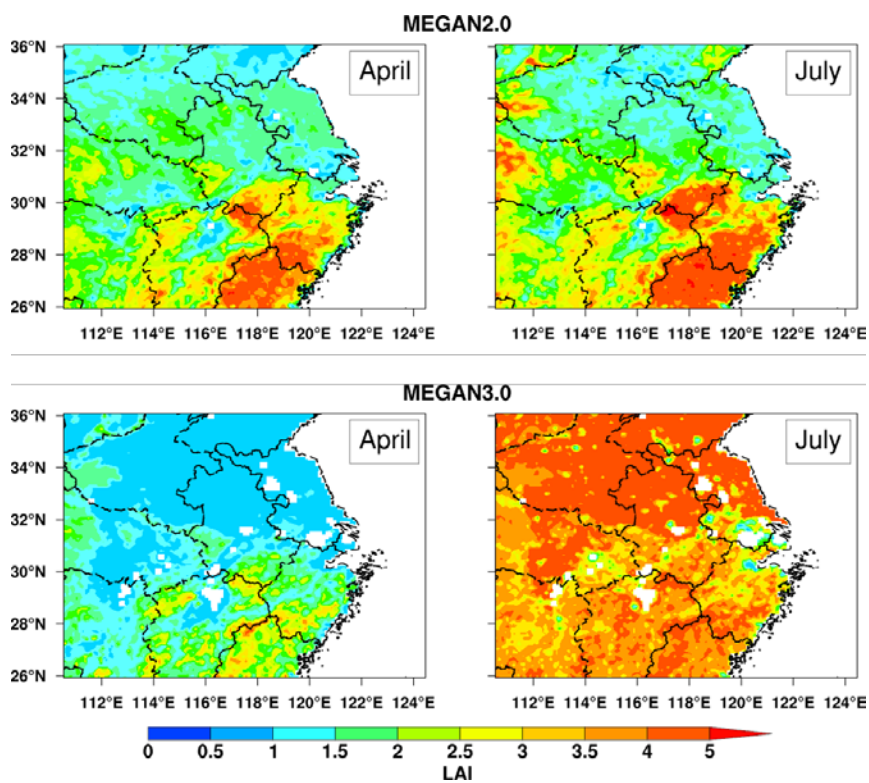
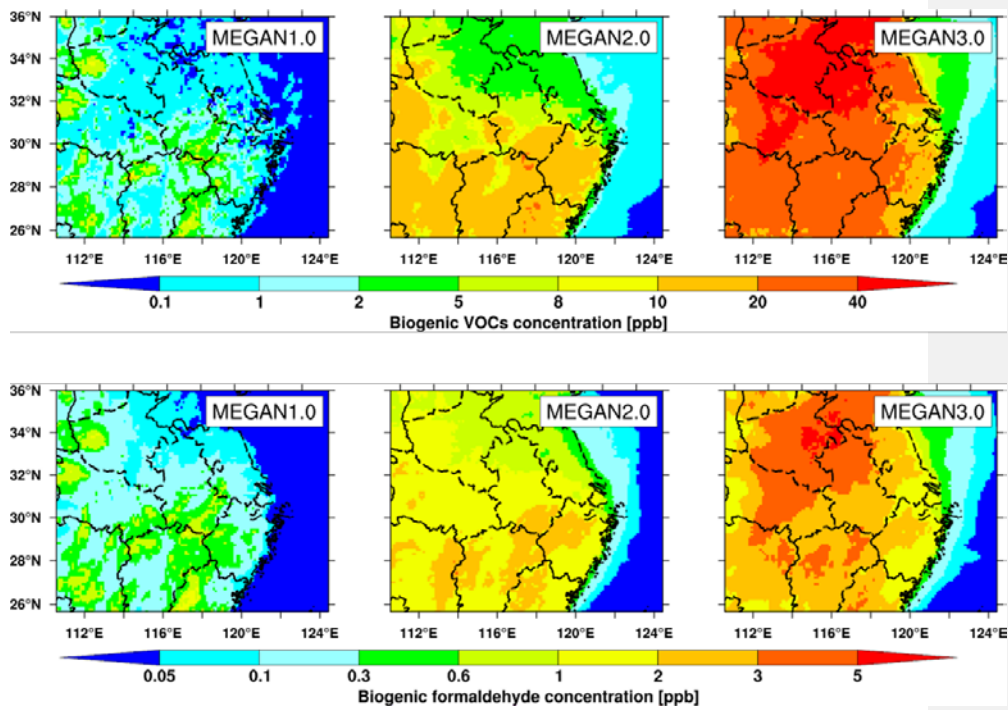


**Figure 9.** The spatial distribution of monthly leaf area index (LAI) from VEG-2015 in the MEGAN v2.0 and MEGAN v3.0.



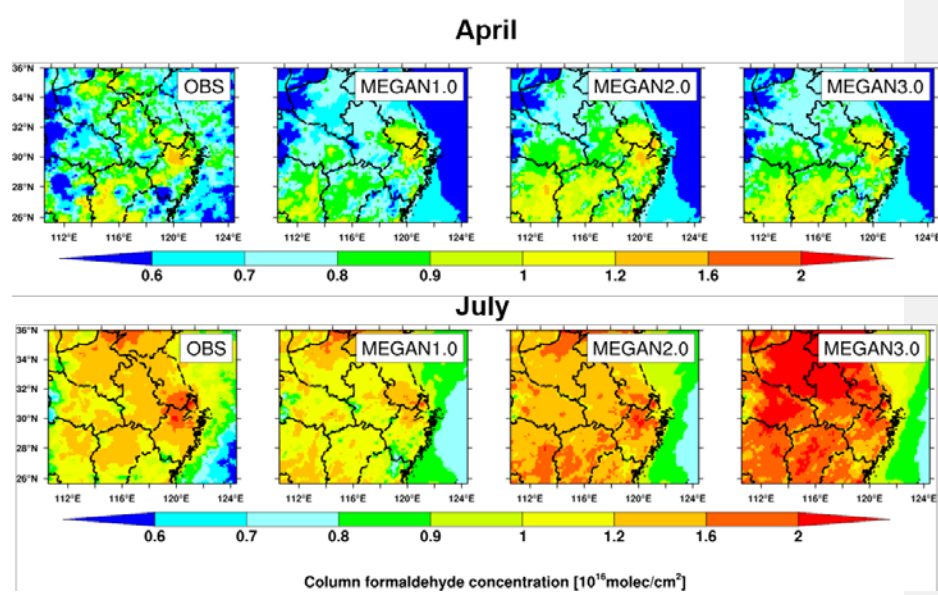
1695  
1696  
1697  
1698  
1699  
1700  
1701  
1702  
1703  
1704  
1705  
1706



1707  
1708  
1709

Figure 10.

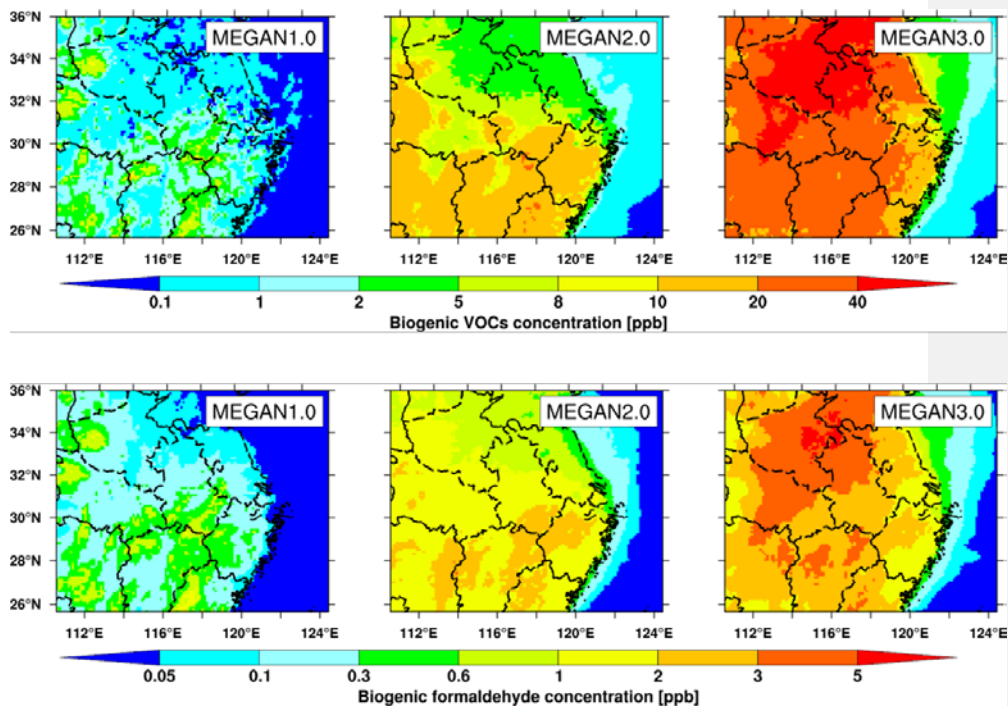
1710



1711 [Figure 10. Spatial distributions of total column tropospheric formaldehyde](#)  
1712 [concentration \(include biogenic and anthropogenic emissions\) in April and July with](#)  
1713 [different versions of MEGAN using the VEG-2015 vegetation date set. The last row](#)  
1714 [is from the satellite retrievals.](#)

1715  
1716  
1717  
1718  
1719  
1720  
1721  
1722

1723



1724

1725 **Figure 11.** Spatial distribution of VOCs and formaldehyde concentration due to the  
1726 biogenic emissions (minus anthropogenic emissions) near the surface in July using  
1727 the VEG-2015 vegetation date set.

1728

1729

1730

1731

1732

1733

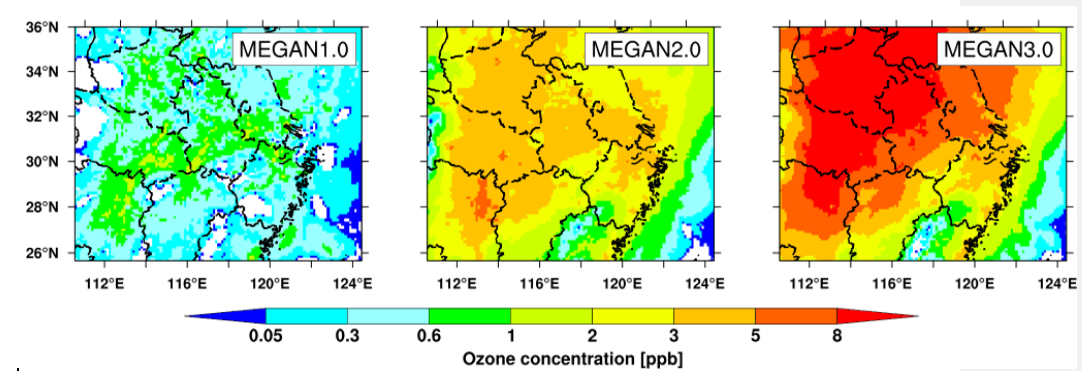
1734

1735

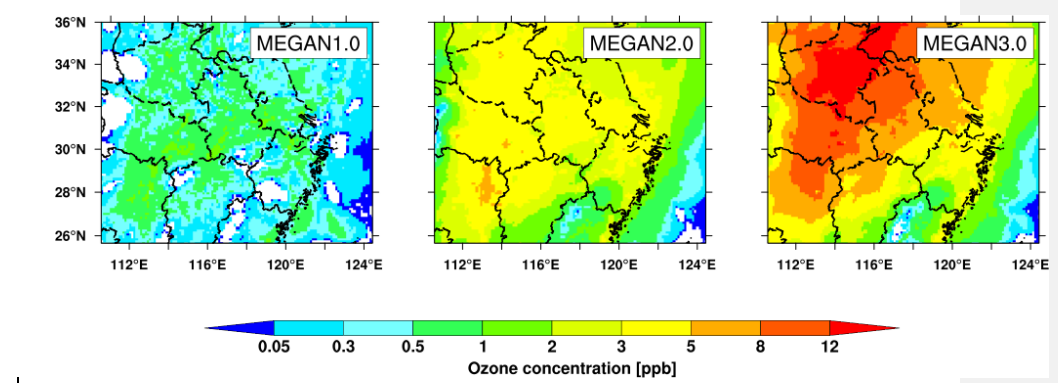
1736

1737

1738  
1739



1740  
1741



1742  
1743  
1744  
1745  
1746  
1747  
1748  
1749  
1750  
1751

**Figure 1742.** Spatial distribution of ozone concentration due to the biogenic emissions near the surface in July using the VEG-2015 vegetation [date set](#) [dataset](#).

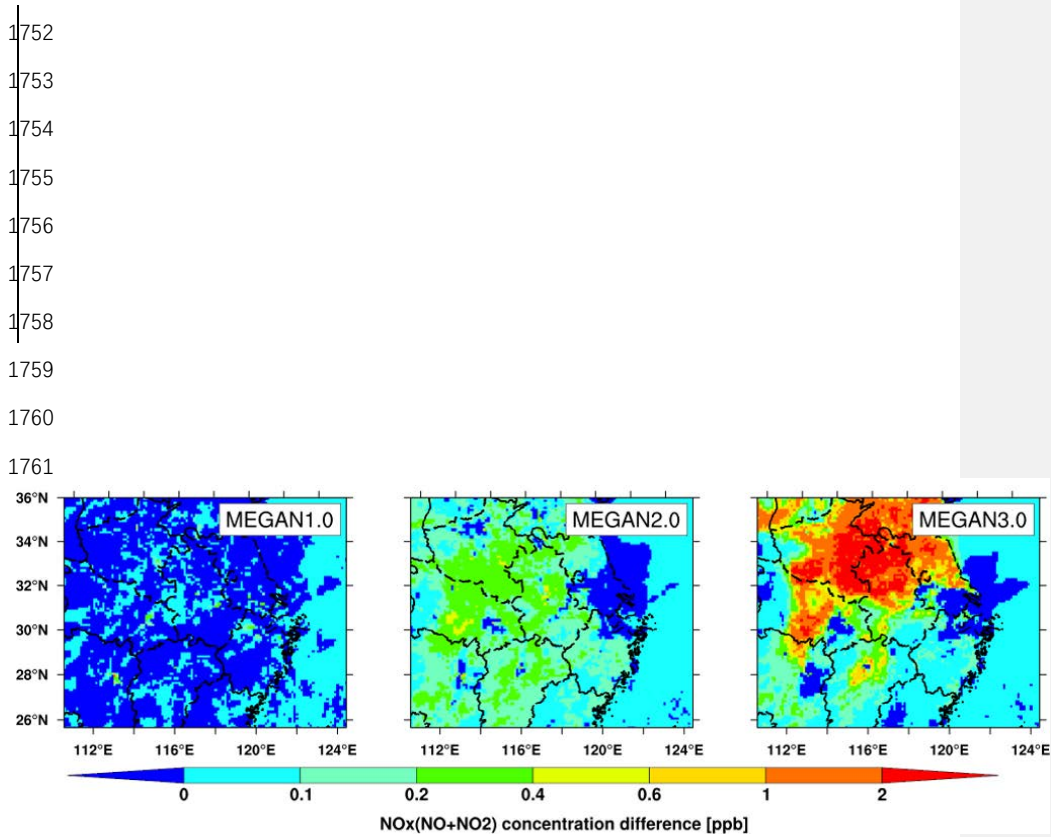


**Figure 1213.** Spatial distribution of NO<sub>x</sub> concentration due to the biogenic emissions near the surface (the difference of simulation considered biogenic emissions and the one without biogenic emissions) in July using the VEG-2015 vegetation date set.

**Table 1** WRF-Chem model configuration

<u>Regions</u>	<u>Eastern China</u>
<u>Domain size</u>	<u>120×100</u>
<u>Simulation period</u>	<u>April and July of 2015</u>
<u>Horizontal resolution</u>	<u>12 km</u>
<u>Gas-phase chemistry scheme</u>	<u>CBM-Z mechanism</u>
<u>Radiation scheme</u>	<u>Fast-J parameterization</u>
<u>PBL scheme</u>	<u>YSU scheme</u>
<u>Microphysics scheme</u>	<u>Morrison two-moment scheme</u>
<u>Surface layer scheme</u>	<u>Monin-Obukhov scheme</u>
<u>Cumulus scheme</u>	<u>Kain-Fritsch scheme</u>
<u>Land-surface scheme</u>	<u>CLM4 scheme</u>
<u>Longwave radiation scheme</u>	<u>RRTMG scheme</u>
<u>Shortwave radiation scheme</u>	
<u>Meteorological initial and boundary conditions</u>	<u>NCEP 1°×1° reanalysis data</u>
<u>Anthropogenic emission inventory</u>	<u>HTAPv2 and MEIC</u>
<u>Biomass burning emission inventory</u>	<u>FINN</u>
<u>Biogenic emission inventory</u>	<u>MEGAN scheme</u>

**Table 2** The domain averaged fraction of PFTs in two vegetation data sets

PFT number	description	VEG-USGS	VEG-2015
0	Bare soil	3.7	6.9
1	Needleleaf evergreen tree–temperature	7.9	1.7
2	Needleleaf evergreen tree–boreal	0	0
3	Needleleaf deciduous tree–boreal	0	0
4	Broadleaf evergreen tree–tropical	0	4.5
5	Broadleaf evergreen tree–temperature	0	0
6	Broadleaf deciduous tree–tropical	0	0
7	Broadleaf deciduous tree–temperature	7.6	4.4
8	Broadleaf deciduous tree–boreal	0	0
9	Broadleaf evergreen shrub–temperature	1.8	0
10	Broadleaf deciduous shrub–temperature	0	0
11	Broadleaf deciduous shrub–boreal	0	0
12	C <sub>3</sub> arctic grass	0	0
13	C <sub>3</sub> grass	0	0
14	C <sub>4</sub> grass	8.7	41.6
15	Crop	70.2	40.8

1799  
1800  
1801  
1802

	Simulation period	BVOC scheme	Vegetation distribution	
			VEG-USGS	VEG-2015
WRF-Chem	April	MEGAN v1.0	Mv1-USGS	Mv1-2015/Mv1-April
		MEGAN v2.0	Mv2-USGS	Mv2-2015/Mv2-April
		MEGAN v3.0	Mv3-USGS	Mv3-2015/Mv3-April
	July	MEGAN v1.0	-	Mv1-July
		MEGAN v2.0	-	Mv2-July
		MEGAN v3.0	-	Mv3-July

1803  
1804  
1805  
1806  
1807  
1808  
1809  
1810  
1811

1812 **Table 23** Numerical experiments of WRF-Chem in this study.

1813  
1814  
1815  
1816  
1817  
1818  
1819  
1820  
1821  
1822  
1823  
1824  
1825  
1826  
1827  
1828  
1829  
1830  
1831

带格式的: 位置: 水平: 11.55 字符, 相对于: 页面, 垂直: 28.95 字符, 相对于: 页面

带格式表格

带格式的: 位置: 水平: 11.55 字符, 相对于: 页面, 垂直: 28.95 字符, 相对于: 页面

带格式的: 字体颜色: 自动设置

带格式的: 缩进: 左侧: 0 厘米, 首行缩进: 0 厘米, 右侧: 0 厘米, 行距: 单倍行距

带格式的: 字体颜色: 自动设置

带格式的: 缩进: 左侧: 0 厘米, 首行缩进: 0 厘米, 右侧: 0 厘米, 行距: 单倍行距



1832  
1833  
1834  
1835  
1836  
1837  
1838  
1839  
1840  
1841  
1842  
1843  
1844  
1845  
1846  
1847  
1848  
1849  
1850  
1851

**Table 34** Measured and simulated isoprene concentrations (ppbv) at sampling sites.

Location and Time	Observation <u>Mean±SD</u>	Simulation (VEG-2015)					
		MEGANv1.0		MEGANv2.0		MEGANv3.0	
		<u>April</u>	<u>July</u>	<u>April</u>	<u>July</u>	<u>April</u>	<u>July</u>
Lishui District, Nanjing ( <u>Apr.2019</u> )	0.062	<u>0.040216</u>	<u>0.071780</u>	<u>0.049098</u>	<u>observation0.518</u>	<u>0.034</u>	<u>0.524</u>
Xujiahui commercial center, Shanghai ( <u>Jan.2007-Mar.2010</u> )	0.120±0.09	<u>≤0.020001</u>	<u>0.075003</u>	<u>0.090097</u>	<u>0.450</u>	<u>0.002</u>	<u>0.037</u>
Northern suburb, Nanjing ( <u>15 May-31 Aug.2013</u> )	0.960±0.56	<u>0.047006</u>	<u>0.905019</u>	<u>0.073114</u>	<u>0.645</u>	<u>0.028</u>	<u>0.367</u>
Nanjing University of Information Science&Technology ( <u>Sep.2011-Jan.2012</u> )	0.300±0.35	<u>0.023009</u>	<u>0.474038</u>	<u>0.480117</u>	<u>0.517</u>	<u>0.067</u>	<u>0.782</u>
Hubei Provincial Environmental Monitoring Center, Wuhan ( <u>Jul.2013</u> )	<u>0.380390±0.480621</u>	<u>0.130004</u>	<u>0.997032</u>	<u>1.0990049</u>	<u>Lyu et al. (2016)0.288</u>	<u>0.025</u>	<u>0.350</u>

1852

1853  
1854  
1855  
1856  
1857  
1858  
1859  
1860  
1861  
1862  
1863  
1864  
1865  
1866  
1867  
1868  
1869  
1870  
1871  
1872

带格式的: 缩进: 左侧: 0 厘米, 悬挂缩进: 2 字符, 首行缩进: -2 字符